

The Effects of Substitution and Doping on Yttrium-based Superconductors

Cameron Danesh-Pajou, Austin Fortino, Sojung Kim, Mahima Kumara, Nancy Lu, Rachel Rizzardi, Maggie Schwabenbauer, and Kai Tinsley

Abstract

Superconductors, materials that have zero resistance, have numerous applications. However, one of the problems that must be overcome is the low critical temperature (T_c). The following research aims to optimize the $\text{YBa}_2\text{Cu}_3\text{O}_{7-x}$ derivatives through both compositional substitutions and doping. X-ray diffraction was run on each sample, followed by resistivity measurements. With the temperature-dependent resistivity, conductivity, X-ray diffraction calculations and effective mass, the mean elastic collision times for the electrons were calculated. Our analysis showed that doping of the yttrium-base with metal oxides, including those of silver and bismuth atoms, was effective in raising the T_c of the samples.

I. Introduction

A. History

The first known superconductor was discovered in 1911 by a Dutch physicist, Heike Kamerlingh Onnes, who found that when a mercury wire was cooled to very low temperatures (around 4 K or -269 °C), its resistivity appeared to vanish. This meant that the material could easily and efficiently conduct electricity for long periods of time. In order to test for full disappearance of the resistance he took a closed circuit of mercury wire and ran a current through it. The current that would normally stop quickly continued as long as the wire was cold. Several decades later, in 1933, Walther Meissner and Robert Ochsenfeld discovered that when a superconductor is placed in a magnetic field, it exudes an equal magnetic field that cancels out the one that is being applied to it. This became known as the Meissner Effect. Over a decade later, in 1957, John Bardeen, Leon Cooper, and John Schrieffer developed the BCS Theory, which describes how materials superconduct at low temperatures. In 1962, Brian D. Josephson discovered that an electric current can flow between two superconductors even if they are separated by a material that does not superconduct, a concept commonly referred to as the Josephson Effect. The 1980s proved to be an extremely progressive decade for superconductors. In 1986 Alex Muller and Georg Bednorz discovered a ceramic superconductor that conducted at a temperature of 30 Kelvin, which was the highest-temperature superconductor at that time. Ceramics are typically very poor conductors, which made Muller and Bednorz's discovery even more interesting.¹ The highest temperature superconductor known to date was discovered in 2014 by researchers at the Max-Planck Institute for Chemistry in Germany, and is a hydrogen sulfide compound placed under extreme pressure, which superconducts at temperatures around 190K.²⁸

B. Recent Experiments

There have not been any major advancements or discoveries in actually creating superconductors at higher temperatures. Most scientists are figuring out theoretical compounds that would work well, but are not testing them. The most common superconductor research is with bismuth compounds and with lead doping. There are numerous elements that would work better but which are impractical because of their harmful qualities. A 2014 study claimed that theoretically, a superconductor could be created at room temperature with infrared laser pulses through the same base compounds used in this project. The recent doping attempts added oxygen to their base compounds with high temperatures similar to how in this project, the base compound was reacted with oxygen.²

A group of researchers substituted bismuth into a $\text{YBa}_2\text{Cu}_3\text{O}_{7-\delta}$ compound and discovered that it superconducted at around 91 K. Their procedure was almost the same as the one used in this project and they had very similar results.²⁹ Another research group in 1994 studied the contact points with silver on a base superconductor. They used the base compound $\text{YBa}_2\text{Cu}_3\text{O}_{7-\delta}$ and it worked as a superconductor as they worked with the resistivity through the silver.³⁰ There is a group that tried to layer the different base compounds and metals to get a higher superconductor with the RABiTS technique. The substance is rolled to a texture like copper, annealed, and layered in a certain pattern to optimize the conducting at high temperatures. Their epitaxial superconductors raised the critical temperature and showed promising results.³¹

C. Applications

Because of their many unique properties and capabilities, superconductors have been applied in many different areas of technology, research and science. Ever since their discovery, possibilities for their use have been explored and developed, and continue to change with time. Primarily because they exhibit zero resistance, have high current-carrying capacities, and can produce extremely strong magnetic fields, their applications have been mainly involved in electricity and magnetism. In addition to these, however, possibilities also exist in areas such as medicine and transportation. Further development and research into these materials could lead to an increase in cost efficiency, convenience of use, and open the door for even more opportunities.

Superconductors are excellent for applications where electrical conductivity needs to be optimized. One major example is power transmission. In the United States, copper wires span hundreds of miles to carry electric power to homes, businesses, streetlights, and many other power-dependent structures. Copper, however, while conductive, is still considerably inefficient at transporting electricity over long distances.³ Much of the energy generated at the power source is lost as heat before it reaches its destination, primarily because copper still exhibits a degree of resistance to current flow. Superconductors offer a much more favorable alternative, capable of transmitting 3 to 5 times more power than copper.³ This increase in efficiency means that more of the generated electricity actually gets used, which cuts costs for energy companies and could also decrease carbon emissions that result from electricity generation. This quality is more pertinent than ever before, as demand for power increases and the current electric grid starts to fail.⁴ Incorporating superconducting materials into the grid would enable a much more efficient and robust power distribution system, as well as potentially save the federal government billions of dollars in rebuilding the current system from the ground up.

As both global trade and the human population increase, efficient manufacturing and transportation are becoming more significant. Superconductors have been at the forefront of various innovations that address

these issues, such as the development of magnetic levitation (maglev) trains (Figure 1). Maglevs use magnetic repulsion to levitate above a track and propel them through the air, allowing them to move with minimal frictional contact with other solid surfaces; they are currently capable of traveling at speeds up to 600 kilometers per hour (kph).³ A strong magnetic field must be generated for this levitation and propulsion, however, and superconductors' high sensitivity to a magnetic field makes them perfect for this application. Additionally, maglevs are more environmentally friendly than other long-distance methods of travel, such as airplanes and trucks, because of their reliance on electricity. Besides maglevs, however, superconductors could be used in other areas of industry and transportation, such as high-power ship motors, industrial motors used in manufacturing, and hybrid vehicles, all of which would result in increased efficiency, production output and flexibility.



Figure 1: Maglev Train in Japan⁵

Ever since the advent of computers and the Internet, the world is becoming increasingly more connected, increasing demands on wireless communication and computational power. For the past few decades, computers have been able to increase their processing power and speed at an exponential rate, but are beginning to reach a point where the continuation of this trend is uncertain. While more transistors, which are at the heart of computing and computer chips, are being packed onto boards to increase speed, the processing speed per transistor currently has not been able to exceed 3 to 4 GHz,³ and technologists can only make them so small before they become impractical. Likewise, use of cellular communication is increasing, and much more demand is being placed on a limited infrastructure. Integrating superconductors into both technologies could help developers and suppliers continue to meet, and even transcend, demand. Because they can transmit more electricity at a faster rate, superconductors would lead to faster processing power (experimental superconductor-based Rapid Single Flux Quantum (RSFQ) circuits have surpassed 20 GHz),³ and a decrease in power consumption for computers, and improve signal quality and range for wireless communication. The rapid advancement of technology, and therefore demand for these innovations, could continue for many more years.

Superconductors have potential applications in areas of scientific research as well. Medicine in particular could benefit through superconductor integration into Magnetic Resonance Imaging (MRI),⁶ a noninvasive, radiation free technology that has allowed doctors to view inside patients. Because they rely on the use of high-power magnets to obtain images, superconductors would potentially increase the precision, power, and stability of the machine, leading to more advanced higher-resolution imaging.³ MRI systems continue to see an increase in use, so improving them would positively impact a growing number of people. Other

areas of scientific research, such as nuclear fusion and particle physics, also require high-energy magnets and electronics that benefit from superconducting materials.

While there are many possibilities and uses for superconducting materials, there are many obstacles and current drawbacks. A major one relates to an innate property within the materials themselves: superconductors only exhibit zero resistance at very low temperatures. As a result, current systems that utilize superconductors must incorporate advanced cooling technology, which can add cost, decrease flexibility, and be difficult to use. More research must be conducted to obtain a better grasp on the properties of these materials and develop them to operate at higher temperatures. This, however, requires more money to be spent, and thus may face further challenges from a economic and policy-making standpoint. If they are further invested in, however, their impact would undoubtedly be significant and further innovate many existing technologies.

II. Literature

A. BCS Theory

The most prominent theory of superconductivity is known as BCS theory, named after American physicists John Bardeen, Leon Cooper, and John Schrieffer. Their theory was first described in 1957 for type I superconductors, which only exhibit superconducting behavior at low temperatures. However, the BCS theory also plays a small role in the mechanism of higher temperature superconductors.⁷

BCS theory is an aggregate of physical phenomena that come together to describe superconductivity. As an electron moves through the crystal lattice of a superconducting material, the surrounding lattice is ever so slightly pulled toward the moving electron. This distorts the shape of the lattice, causes a momentary partial positive charge, and attracts another electron. These two electrons, called a Cooper pair (Figure 2), can then condense into the ground state, and will show signs of slight attraction. The Cooper pair behaves as a boson, allowing two electrons to occupy the same quantum state. The Cooper pair has a slightly lower energy than the individual electrons, causing a lower frequency of collisions as it moves through the crystal lattice. This, along with the fact that the other atoms in the lattice are moving slower due to their low temperature, leads to a lower resistivity.

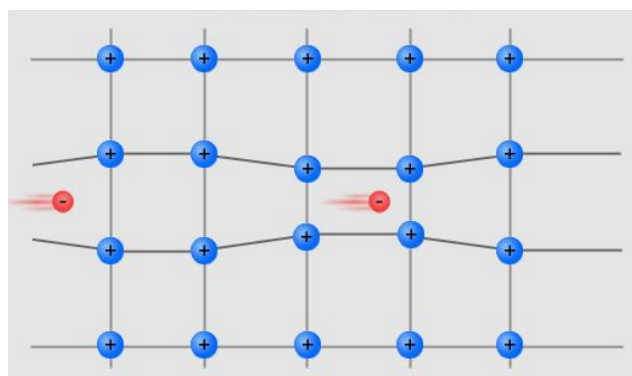


Figure 2: Cooper Pair⁷

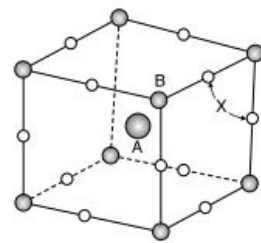
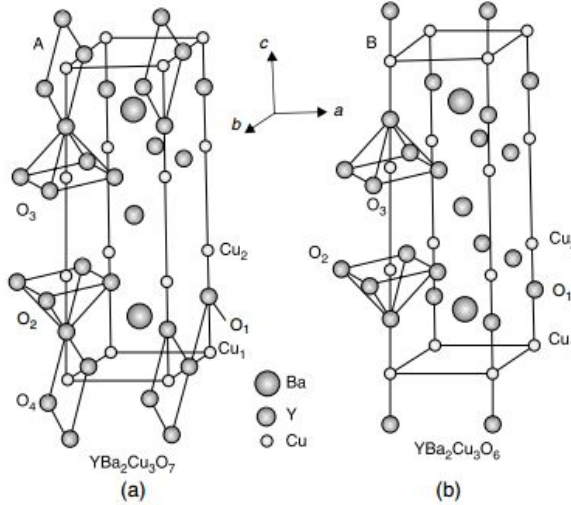
However, at higher temperatures, an event called a phonon interaction or thermal vibration occurs continuously throughout the crystal lattice. As the temperature of the crystal increases, the constituent

atoms begin to vibrate faster causing a higher resistivity. The strength of these vibrations determines how well the Cooper pair can stay bound. If the phonon interactions are too vigorous and unsettling for the electrons, i.e. if the temperature is too high, then the low energy bond of the Cooper pair will be broken, and superconductivity will not occur.⁸

BCS theory describes superconductivity for low temperature superconductors very well. However, high temperature superconductors appear to operate on a significantly different basis. The rationale behind Cooper pair interaction comes from the thermal energy of the lattice being low enough for Cooper pairs to condense and allow for zero resistance. A logical assumption can be made; BCS theory does not explain high temperature superconductors like those studied in this experiment. The leading theory on high T_c superconductors with orthorhombic symmetry is based on empirical data about how much oxygen is in the compound. Specifically, it is believed that conduction occurs in CuO_2 planes which disappear when there is not enough oxygen.⁹

B. Theory Behind Substitution and Doping

The yttrium barium copper oxide ($\text{YBa}_2\text{Cu}_3\text{O}_{7-x}$) superconductor is one of the most common high-temperature superconductors. Known more commonly as a 1-2-3 base (reflecting the ratio in which the three metal elements are combined), it superconducts at a relatively high temperature of 92K. The crystal structure of the 1-2-3 is important to its conductivity, essentially comprising of layered sheets of copper and oxygen atoms (characteristic of all cuprate superconductors) alternating with sheets of barium and yttrium atoms. In the completed compound, there are about seven oxygen atoms per unit cell (See Figure 3). The variability in oxygen is crucial to the superconductivity, as the copper oxide (cuprate) layers are those that actually give rise to superconductivity. Between the superconducting cuprate planes, a heavy metal element resides in the body center of the unit cell to provide stability. The main superconducting plane is surrounded by layers formed by oxygens and another alkaline earth metal or rare earth metal; in the instance of the 1-2-3 base, the heavy element residing in the body center of the conducting plane unit cells is yttrium while the other metal is barium.¹⁰ Although the structure of the unit cell can accommodate a maximum of nine oxygen atoms, there must be seven or less oxygen atoms per unit cell for the compound to superconduct, and the amount of oxygen added is variable because of the dependency on the firing process. However, if the molar coefficient of oxygen in the compound is less than 6.5 overall, the compound will not superconduct. The lack of full oxygen saturation leads to vacancies in the lattice that happen in specific places, namely the copper oxide planes, which gives rise to odd oxidation states of the copper atoms (seemingly significant for superconductivity). The 1-2-3 base compound is a derivative of an ideal perovskite with an oxygen deficit, and has an orthorhombic structure. The lattice structure consists of two CuO sheets in the ab -plane and $\text{Cu}-\text{O}$ chains along the b -axis. The specific presence of oxygen in the structure is essential for superconductivity.¹¹

Fig. 2.1. The perovskite structure ABX_3 Fig. 2.2. The structure of YBCO (a) orthorhombic structure ($a_0 = 3.823 \text{ \AA}$, $b_0 = 3.885 \text{ \AA}$, $c_0 = 11.7 \text{ \AA}$) (b) tetragonal structure ($a_0 = b_0 = 3.86 \text{ \AA}$, $c_0 = 11.7 \text{ \AA}$)Figure 3: Unit Cell and Crystal Structure of $\text{YBa}_2\text{Cu}_3\text{O}_{7-x}$ ¹²

1. Substitution

In order to study superconductors, it is possible to substitute in different elements for elements in the base compound in an attempt to create a novel product which could potentially also superconduct at a higher temperature. Because the layers in the crystal structure are crucial to the superconducting abilities of cuprate superconductors (probably need a source), the main goal of the substitutions was to substitute in elements that would preserve the unit cell crystalline structure of the original 1-2-3 base. Elements of similar oxidation states and sizes to any of the original metallic elements could be considered as possible substitution candidates.

2. Doping

Doping is a process in which elements are added into the spaces in the crystal lattice structure of the base compound; instead of adding one element in place of another as in substitution, a very small amount of a separate element is added to the preformed base mixture in an attempt to create a solid solution in which the dopant fits into the holes in the lattice without disturbing the original structure of the 1-2-3 base. For the base to be successfully doped, the dopant must be small and non-intrusive (it must fit into the spaces of the crystal lattice).

C. X-Ray Diffraction

An important aspect of analyzing superconductors is understanding and determining their crystal lattice structure. The structure of compounds have a significant impact on their electrical conductivity, as it dictates where electron orbitals are located among the atoms and ions of the solid. For example, metals are excellent conductors because when their atoms form metallic bonds, they draw so close together that their outermost energy levels form high-energy conduction bands that allow current to flow. Because the bands are empty, and the atoms are so close together, valence electrons are easily excited into the bands and move throughout the whole material.¹³ Insulators, on the other hand, usually form covalent bonds, where electrons are shared. Thus, their atoms are further apart and their outer energy levels are more likely to be filled. Comparing the lattice of different superconducting materials aids in identification of physical and structural properties that may be more favorable and can lead to a more complete understanding of how these materials work.

Since superconductors have a crystal lattice structure, they can be analyzed through a process called X-ray diffraction. X-rays are a form of electromagnetic radiation, and thus can be characterized as waves when travelling through space. When these waves collide with atoms in the crystal, they are reflected in different directions.¹⁴ Diffraction is a process that relies on the positions of atoms in crystal lattice and their interaction with these waves, and employed using a diffractometer.

For x-ray diffraction to occur, the wavelength of the waves emitted must correspond with the spacing of the layers of atoms in the lattice. These waves are directed at a thin layer of solid as an intense beam. The angle of this beam, represented by θ , is then reflected back at an angle of 2θ and registered by a detector. Thus, the beam emitter is placed at an angle of θ with respect to the solid and the detector is placed at an angle of 2θ .¹⁵ If the plane that atoms are placed on are a certain distance apart, the waves reflect back in phase, resulting in constructive interference and a more intense beam. If that distance is halved, or the angle is changed, then the waves reflect back out of phase and the result is destructive interference. The x-ray diffractometer rotates the angle of this beam over the crystal solid, and the subsequent states of the reflected waves are used to analyze and determine the position of the atoms in the lattice. This relationship can be represented by Bragg's Law, $n\lambda = 2dsin\theta$ ¹⁵, and is illustrated in Figure 4.

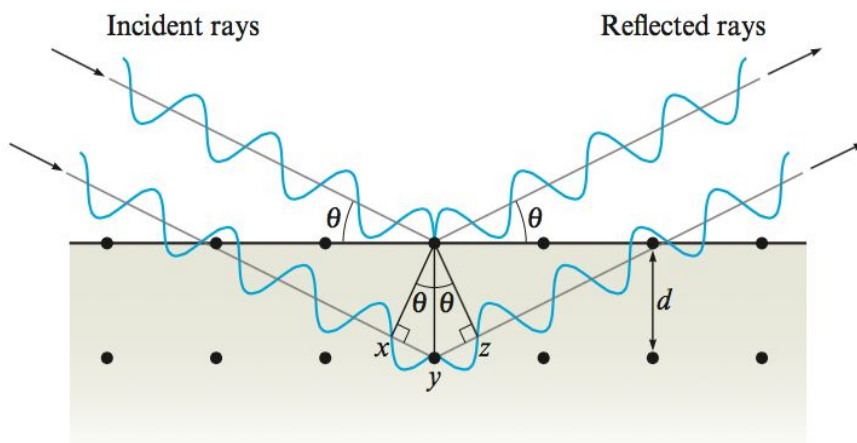


Figure 4: X-Ray Diffraction on a Crystal Lattice ¹⁴

D. Resistivity

The most distinctive property of superconductors is their lack of resistance below the critical temperature (T_c), a point where resistance suddenly drops very quickly. As a result, certain phenomena can begin to occur. For example, a current can run for an infinite amount of time through a superconductive loop. Electrons have formed a new quantum collective state, where collisions, while still existent, no longer cause electrical resistance.¹⁶ Currently, there are no superconductors that exist at temperatures close to easily created environments. The search to find a superconductor with a high T_c is crucial to make widespread application of the principles possible.

Resistance, an extrinsic property, is defined as the loss of energy in the form of heat due to passage of electrical current. Electrical resistance depends on both the length and the cross-sectional area of a wire. Resistivity, on the other hand, is an intrinsic property. The equation used is:

$$R = \rho L/A$$

where R represents resistance, L represents length, A represents cross-sectional area, and ρ represents resistivity.¹⁷ Resistivity was used in this experiment because the samples were of different sizes, which would have affected the resistance readings. Zero resistivity corresponds to perfect diamagnetism, which by the Meissner Effect, allows the material to exclude any magnetic field. In particular, the type II superconductors exhibit a mixed-state Meissner Effect, which has not fully been explained in terms of quantum states.

III. Procedure

A. Determining Materials for Substitution and Doping

Because yttrium is the metal atom in the middle of the two superconducting CuO_2 planes, substitutions for yttrium were done because it was hypothesized to have the most direct impact on superconductivity. First, potential substitutes for yttrium were researched and identified. The substitutes were required to have the same charge as yttrium (+3) and a similar atomic radius (the atomic radius of Yttrium is 2.12 Å). This ensured the desired bonding pattern, both ionically and to preserve the crystal structure of the base superconductor. Also, potential dopants for the base compound, $YBa_2Cu_3O_{7-x}$, were identified. These dopants were chosen based on size (their atomic radii had to be small enough to fit within the lattice holes of the compound) and availability.

Two samples of the base compound, $YBa_2Cu_3O_{7-x}$, were made, using yttrium (III) oxide, barium (II) oxide, and copper (II) oxide. Oxygen gas was added later, during firing of the powders into a pellet. The oxide powders were massed out and mixed in the necessary stoichiometric ratios to create a 5-gram pellet after adding the oxygen and firing (see “II. Preparation of Samples” for details).

Next, several substitutions were carried out, three full and one partial. Full substitutions for yttrium were carried out with dysprosium, samarium, and neodymium individually, and a partial substitution was carried out with equal molar amounts of dysprosium, samarium, and neodymium. Additionally, samples of the base compound were doped with a small amount of various elements. The dopants were added in a ratio of .1

moles per mole of compound, except for bismuth and indium, which were added in a ratio of 0.2 moles per mole of compound. Five compounds were created, each one doped with one of bismuth, gallium, tin, silver, and indium. Finally, a compound was created with a mixture of yttrium (III) oxide and two barium-calcium-copper compounds, $\text{Ba}_2\text{Ca}_2\text{Cu}_2$ and BaCaCu_2 .

See Tables 1 and 2 for details on all materials made.

Table 1: Substituted Samples

Substituted Element	Compound	Charge of Element	Atomic Radius (\AA)	Ionic Radius (\AA)
Yttrium (base compound)	$\text{YBa}_2\text{Cu}_3\text{O}_{7-x}$	+3	2.12	1.04 - 1.215
Dysprosium (Dy)	$\text{DyBa}_2\text{Cu}_3\text{O}_{7-x}$	+3	2.28	1.04 - 1.215
Samarium (Sm)	$\text{SmBa}_2\text{Cu}_3\text{O}_{7-x}$	+3	2.38	1.052 - 1.223
Neodymium (Nd)	$\text{NdBa}_2\text{Cu}_3\text{O}_{7-x}$	+3	2.06	1.098 - 1.38
Dy, Sm, Nd	$\text{Dy}_{1/3}\text{Sm}_{1/3}\text{Nd}_{1/3}\text{Ba}_2\text{Cu}_3\text{O}_{7-x}$	+3	Dy - 2.28 Sm - 2.38 Nd - 2.06	1.123 - 1.41

Table 2: Doped Samples

Element Doped	Compound	Atomic Radius (\AA)	Ionic Radius (\AA)
Bismuth	$\text{YBa}_2\text{Cu}_3\text{O}_{7-x} + \text{Bi}_{.2}$	1.43	0.55 - 0.81
Gallium	$\text{YBa}_2\text{Cu}_3\text{O}_{7-x} + \text{Ga}_{.1}$	1.36	0.61 - 0.76
Tin	$\text{YBa}_2\text{Cu}_3\text{O}_{7-x} + \text{Sn}_{.1}$	1.45	1.00 - 1.28
Silver	$\text{YBa}_2\text{Cu}_3\text{O}_{7-x} + \text{Ag}_{.1}$	1.65	0.76 - 1.06
Indium	$\text{YBa}_2\text{Cu}_3\text{O}_{7-x} + \text{In}_{.1}$	1.56	1.10 - 1.31

B. Preparation of Materials

1. Stoichiometry

In order to get a five gram sample of the $\text{YBa}_2\text{Cu}_3\text{O}_{7-x}$ compound, 0.00750 moles of the base compound was required. This value was used to calculate the number of moles of each element required to make the desired base. After calculating the number of moles needed for each element, that value was converted into the number of moles of the oxide needed to make the base. Then, using the molecular mass of each of

these oxides, the number of moles of oxide was converted into grams so it could be massed out to be mixed into the compound. For the substitutions, the moles of the base compound was used to calculate the grams of the substituted oxide needed to produce a five gram sample while still maintaining the same 1:2:3 ratio. For the partial substitution the moles of yttrium needed was divided into thirds and was used to calculate how many grams of each oxide being substituted. After using all of the BaO, Ba₂CaCu₂O₅ and Ba₂Ca₂Cu₃O₇ needed to be used to calculate the correct amount of barium and copper needed to make the compound while minimizing the amount of calcium added. When doping, 10% of the moles of the base compound was calculated and then converted into grams of the specific oxide of the element that was being doped.

2. Mixing

After the mass needed was calculated for each chemical oxide, each oxide was massed out individually to make each sample and mixed thoroughly with a ceramic mortar and pestle so that the mixture was homogeneous throughout. Because the powders were so fine, a mortar and pestle were necessary to make sure everything was thoroughly mixed. This was done for each individual sample to prepare the samples for firing.

3. Firing

The mixtures were fired in a tube furnace in two sequences. First, the powder mixture was transferred into an alumina ceramic boat, then fired according to the following temperature sequence: heat up to 80°C, hold at 80°C for 10 minutes, heat for 4 hours until reaching 850°C, heat for 2 hours until reaching 960°C, hold for 8 hours, cool for 9 hours until reaching 200°C, then cool to 0°C. After this first firing, the mixture was reground and pressed in a hydraulic press, then fired again in its pellet form according to the same temperature sequence.

4. Pressing

Each sample made had to be pressed before being analyzed. After firing the sample was loaded into a mold that had a small rod in the bottom to hold the sample in. After the sample was placed into the mold another longer rod was slid in the top of the mold and put into the press. In order to get the sample to be a uniform size and shape the pressure had to slowly be increased to a total pressure of 25,000 psi. If the pressure was increased too quickly, the sample would not form correctly and could crumble after it was taken out of the mold. After increasing the pressure to the desired value the mold was removed from the press and the sample was extracted from the mold and then taken to be fired for the second time.

5. Cutting

After the second firing process, the pellets were sent to the diamond saw to be cut. First, a narrow piece was cut from the edge of the pellet and sent to the x-ray diffraction analysis lab to be crushed into a fine powder with a mortar and pestle. Next, another cut was made to form the first side of a two millimeter bar of about three quarters of an inch in length. Finally, a last cut was made to form the bar that would be used for resistivity analysis. After the last cut, the bar was wiped clean to remove any contaminating dust, and was inspected thoroughly for burrs and cracks. The weight of the apparatus would often force the bar to break off before the saw could cut the pellet precisely, and as a result, burrs would form along the corners of the bar. Fine grit sandpaper and a simple razor blade were used to remove the burrs. If there was a

major crack in the bar there were two options available: Either place the silver contacts used for resistivity analysis on the side of the bar that has no visible crack, or cut a wider bar from the remaining pellet so the silver contacts can fit on the side without the crack. For example, a crack was found in sample number five. This was not a severe crack, and the face that did not show the crack was sufficiently wide enough to have the contacts fit. However, in sample number six, there was a crack that destabilized the integrity of the bar. This was fixed by using the razor blade to trim the width of the bar so that the crack was no longer an issue. Altogether, there was no pellet that could not ultimately endure the cutting stage.

The pellets needed to be cut with a diamond saw blade because they are too hard to be cut by common materials such as steel or brass. Diamond is at ten on the Mohs hardness scale, while many ceramics are around seven, and steel is close to six.¹⁸ Even with a diamond blade, all three cuts for one pellet took approximately one hour on average. This is a result of a meager amount of force applied to keep the pellet on the blade. If the force applied to the sample on the blade is too much, the pellet may fracture or shatter.

Dust from the previous samples would occasionally clog and saturate the spaces between the diamond particles that cover the edges of the blade. A dirty blade could escalate cutting time by as much as five minutes for one cut. To avoid this gratuitous increase in cutting time, a soft material was used to clean the blade. This material was held against the blade and make a shallow cut into the side of the soft substance. It was crucial to be sure that no dust from the cleaning material contaminated the dust from the samples. If there was dust from the cleaning substance mixed with the dust from the superconductor, the x-ray analysis data would be rendered useless. Furthermore, it was paramount to have a steady hand when cleaning the blade. If control of the cleaning material had been lost, the blade could have been irreparably damaged.

C. Resistivity Testing

In order to test the resistivity of the sample, measurements such as current, temperature, and resistance must be taken. A thermocouple placed between a container filled with ice water and the sample, which was located in a vacuum-sealed tube connected the devices. This was used to gather temperature readings, which, when combined with amperage and resistance were used to calculate resistivity.

For each of the cut samples, four strips of silver silicone-based paint were applied. The sample was placed into an apparatus such that the silver was aligned with the metal contacts to ensure that the current ran smoothly. The sample was then placed in a glass tube which was then sealed with a ring (Figure 5). First, the containment vessel was flushed with helium to remove any moisture or air. It also provided both a conductive environment and an inert environment. After the flushing, the sample was physically lowered into a dewar of liquid nitrogen until the temperature was approximately 110 Kelvin. The temperature rate of decrease was then adjusted by changing the height of the tube in the nitrogen to approximately 0.3 degrees/minute. The cooling process from 110 to 80 Kelvin was recorded as part of a cooling curve. The reverse process was used to obtain a heating curve afterwards. The heating process was easier to control and therefore yielded more data points and therefore a more accurate curve. Five trials were obtained for each of the twelve samples with varying amounts of resistance (to create 1, 5, 10, 20 and 50 mA of current.)²²

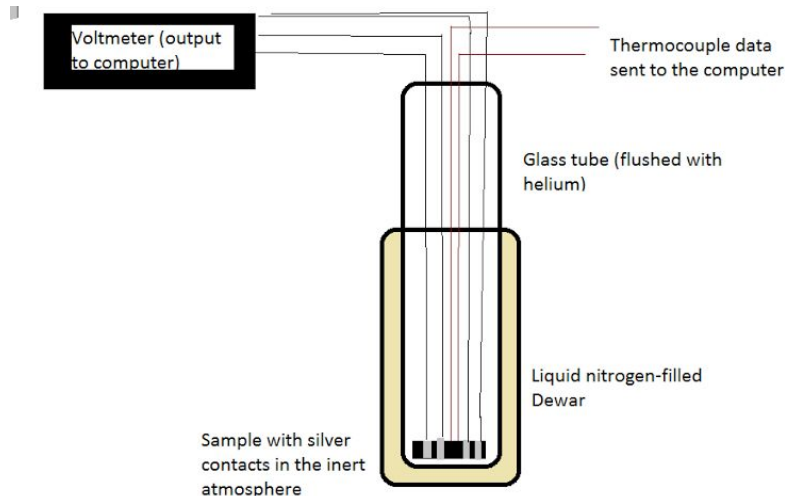


Figure 5: Experimental Setup for Testing the Resistance

The overall circuit consisted of a variable resistor with five possible resistances, a battery, several switches and a sample as well as a measuring apparatus (voltmeter). The variable resistor allowed five different currents to run through the sample to test for superconductivity. For the temperature measurements, a thermocouple was attached to the sample and to an ice-water bath (not shown above) to measure the thermal gradient.

If, when current was increased, after a certain level of current, there was no change in resistance, this indicated that a sample superconducted. Generally, it was possible to collect data indicating that the resistance of the sample actually reached zero. However, even if it did not reach zero, a constant resistance as current was increased still indicated superconductivity.

D. Determination of Crystal Structure: X-Ray Diffraction

A compound's structure has an impact on how and whether it superconducts, so analyzing the solids using x-ray diffraction was an important component of the experiment. Because it is already verified that $\text{YBa}_2\text{Cu}_3\text{O}_{7-x}$ superconducts, its lattice structure, for the purposes of this experiment, was considered to be optimal for superconducting. Thus, the x-ray pattern of each of the doped and substituted compounds for the purpose of comparing it to the 1-2-3 compound and determining to what degree the structure changed. Presumably, the less warped the structure, the more likely it is to superconduct. However, since the goal of the experiment is to change the 1-2-3 compound's superconducting properties by increasing its critical temperature, this is not considered to be a rule.

X-ray diffraction works by aiming an intense x-ray beam at a thin slide containing a powdered layer of the solid to be analyzed. This beam is directed at an angle of θ at the slide, and is diffracted off at an angle of 2θ , which is picked up by a detector. A diffractometer aims this continuous beam at the solid, and rotates slowly around it, so that the intensity of the diffracted waves can be compared to the angle of the beam, which provides a more 3-dimensional description of the structure. Through this, the crystal structure and lattice parameters of the solid can be determined.

For this experiment, a Siemens D500 X-ray Diffractometer (Figure 6) was used to obtain the data of the solids' structure. This model emits copper K-alpha x-rays (which have a wavelength of 1.52 Å) and communicated with the computer through an MDI Databox Interface. The Databox then interacted with the MDI Scanner 5 program (Figure 7), which maps the intensity of the diffracted waves as peaks with respect to the value of 2θ .



Figure 6: X-ray Diffractometer¹⁹

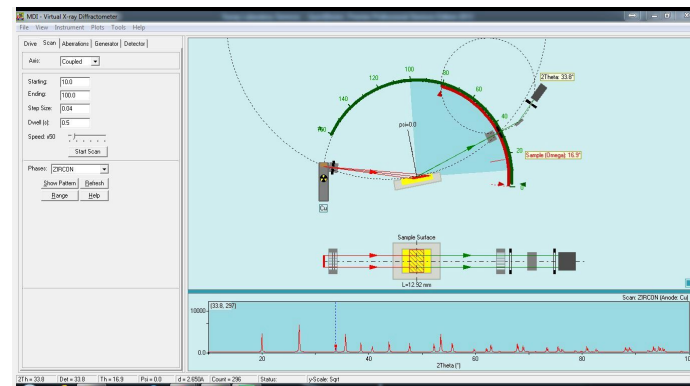


Figure 7: MDI Scanner Program²⁰

Before inserting a sample into the diffractometer, the sample needed to be ground into a fine powder to place on the x-ray slide. This was accomplished by using a mortar and pestle on a small piece from the compound's pellet and mixing the grains with the shavings generated by the diamond saw used in cutting. Grounding the compounds helped ensure a random orientation of crystals on the diffraction plane, which would help keep the peak values consistent. Dow Corning high vacuum silicone grease was then applied to the slide and thin layer of the powder was applied over it to keep the solid in place. Excess solid was removed by gently tapping the sides of the slide. Then, to ensure the grease held the particles firmly in place without being smeared, a small sheet of glass was used to press the particles onto the grease. If the grease became smeared, the solid particles would be covered in the grease and change the diffraction data. The glass was then removed and any remaining excess adhered to its surface.

The D500 diffractometer then needed to be powered to the correct settings. The water supply, which was used to cool the x-ray beam emitter, was set to 70 psi, and the voltage and current set to 40 kV and 20 mA, respectively. The slide could then be set into machine and the beam shutter opened. For superconductor samples, intensity peaks are mapped between a 2θ range of 20.000° to 80.000°. So, using the MDI Scanner 5 program, the machine would be preset to an initial 2θ value of 20.000° and a subsequent θ value of 10.000°. Finally, a preprogrammed procedure designed for 123 compounds was selected in the program and executed, taking the diffractometer from 20.000° to 80.000°, taking roughly 40 minutes to complete. The results were saved a graph generated by the MDI Scanner 5 program. After each scan, the shutter was closed, the sample removed, the slide cleaned, and the 2θ orientation reset.

To analyze the data collected from the diffractometer, the peak maps were transferred to another program called Agilent VEE. Agilent VEE allows the user to create programs customized to plot the peaks of different solid compounds, and thereby obtain their lattice parameters. These lattice parameters can then be used to calculate the volume of each compound's unit cell and compare structures.

A prewritten Agilent VEE program designed to analyze superconductors was used for this experiment. First, the data points were imported, and then basic information about the compound, crystal class, whether it's

a 123 compound, a, b, and c parameters, body/face-centered orientations, and maximum h, k, and l values, are entered. In this case, the entered crystal class was orthorhombic, and the lattice parameters were used from results of prior experiments. The program would then output a peak graph with markers indicating where the most intense peaks, areas of constructive interference, were. In order to fit these markers to the data more precisely, peaks dependent on only one of the hkl planes were identified. Because the *hkl* indices correspond to the abc parameters, respectively, a peak dependent on the *h* index was modified by altering the *a* lattice parameter, etc. If the marker was to far to the left for that peak, the corresponding lattice parameter was decreased while if the marker was to far to the right, the corresponding lattice parameter was increased. Once these markers were fitted, the remaining markers would adjust to their respective peaks.

In addition to scanning the superconductor compounds, the crystal structures of the metal oxides doped into those compounds were also scanned. The method of obtaining the metal oxides' peaks was identical to that of obtaining the other compounds', but fitting the data was slightly different. Because the metal oxides each belonged to different crystal classes and had different lattice parameters, their characteristics needed to be separately researched and analyzed (Table 3). Note that lattice parameter values are approximations and often vary over at least a hundredth of an angstrom.

Table 3: Crystal Class and Lattice Parameters of Metallic Oxide Dopants (from literature)

Solid	Crystal Class	a Value (Å)	b Value (Å)	c Value (Å)
β -Ga ₂ O ₃ ^{21, 22}	Monoclinic	12.23	3.04	5.8
SnO ²³	Tetragonal	3.8	3.8	4.836
In ₂ O ₃ ²⁴	Cubic	10.117	10.117	10.117
Ag ₂ O ²⁵	Cubic	4.723	4.723	4.723
α -Bi ₂ O ₃ * ²⁶	Monoclinic	5.848	8.166	7.51
β -Bi ₂ O ₃ * ²⁶	Tetragonal	7.743	7.743	5.631

* For this experiment, both α -Bi₂O₃ and β -Bi₂O₃ were used as the same dopant.

After all of the lattice parameters were determined, they could be compared and used to calculate the cell volume of each compound for analysis.

IV. Results

A. Resistivity and Temperature

Table 4: Superconducting Temperatures of Compounds

Sample	Temperature (K)
$\text{YBa}_2\text{Cu}_3\text{O}_{(7-x)}$ (#1)	92.2
$\text{YBa}_2\text{Cu}_3\text{O}_{(7-x)}$ (#2)	91.9
$\text{DyBa}_2\text{Cu}_3\text{O}_{(7-x)}$	89.9
$\text{SmBa}_2\text{Cu}_3\text{O}_{(7-x)}$	91.8
$\text{NdBa}_2\text{Cu}_3\text{O}_{(7-x)}$	Superconducts at lower temperatures*
$\text{YBaCaCu}_3\text{O}_{(7-x)}$	Superconducts at lower temperatures*
$\text{Na}_{1/3}\text{Sm}_{1/3}\text{Dy}_{1/3}\text{Ba}_2\text{Cu}_3\text{O}_{(7-x)}$	Does not superconduct
$\text{In}_{(0.2)}\text{YBa}_2\text{Cu}_3\text{O}_{(7-x)}$	Superconducts at lower temperatures*
$\text{Ag}_{(0.1)}\text{YBa}_2\text{Cu}_3\text{O}_{(7-x)}$	93.6
$\text{Bi}_{(0.2)}\text{YBa}_2\text{Cu}_3\text{O}_{(7-x)}$	94.4
$\text{Ga}_{(0.1)}\text{YBa}_2\text{Cu}_3\text{O}_{(7-x)}$	86.5
$\text{Sn}_{(0.1)}\text{YBa}_2\text{Cu}_3\text{O}_{(7-x)}$	91.4

*These temperatures are too low to accurately measure with the devices used. Liquid helium would be necessary instead of liquid nitrogen in order to obtain an accurate measurement, as these materials superconduct at sub-77 K temperatures.

B. Determination of Crystal Structure

1. Substituted Compounds

The peak graphs of the substituted compounds were all very similar to the standard yttrium compound's structure. This implies that the crystal lattice did not experience an extremely major shift in unit cell size. The peak maps of the crystal lattice for the substituted compounds is shown in Figure 8, with the standard yttrium compound on the bottom. Figure 9 shows also shows the graph of the Dysprosium substituted compound, which is not included in Figure 8.

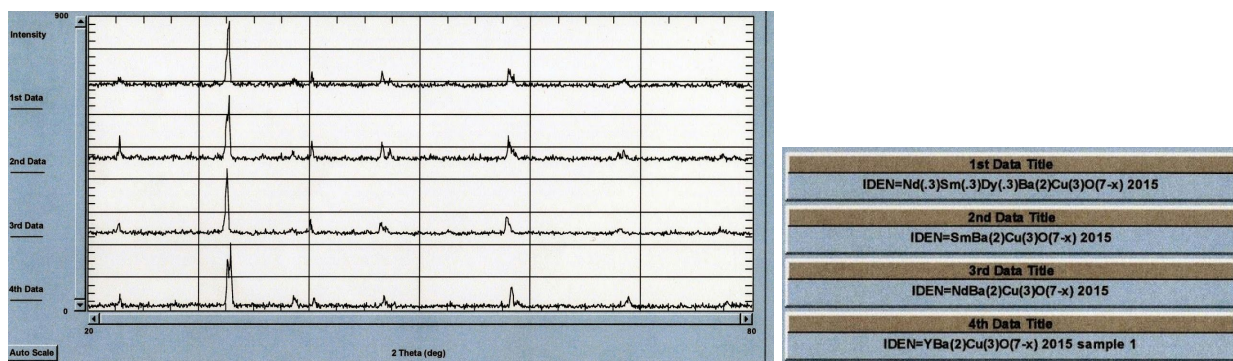
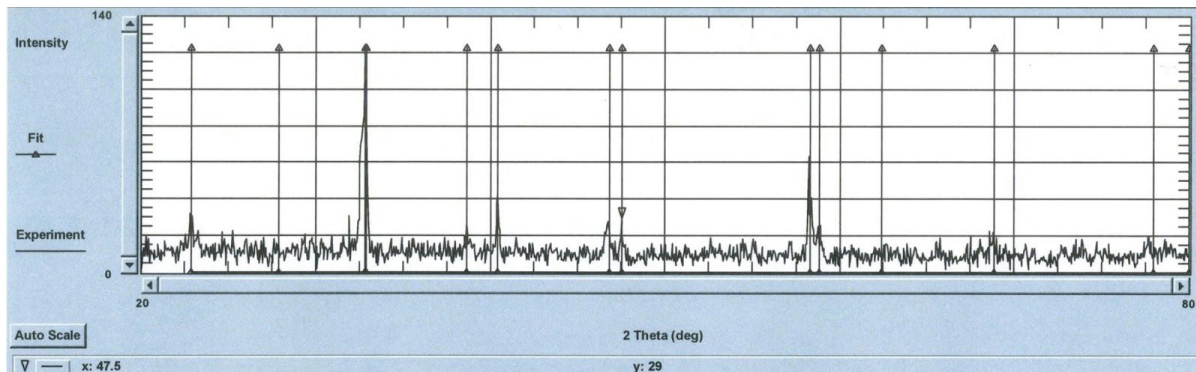


Figure 8: X-ray Diffraction Multiplot of Substituted Compounds**Figure 9: X-ray Diffraction Plot of $\text{DyBa}_2\text{Cu}_3\text{O}_{(7-x)}$**

While the major peaks exist for each substituted compound, they exist in slightly varying intensities. For example, the samarium substituted ($\text{SmBa}_2\text{Cu}_3\text{O}_{(7-x)}$) compound has a relatively intense peak at a 2θ angle of around 23° , while the ($\text{Nd}_{1/3}\text{Sm}_{1/3}\text{Dy}_{1/3}$) $\text{Ba}_2\text{Cu}_3\text{O}_{(7-x)}$ compound has an extremely weak one. These intensities, however, do not necessarily dictate how similar to the base compound the crystal is. In order to maintain consistent results, the crystals' orientations must be completely randomized, which is why the sample is ground into powder. However, this can never be perfectly achieved, meaning that some particles will maintain a specific orientation and x-ray plots will often have varying intensities for the same peak. The component of major importance in these diagrams is *where* the peaks are located, as this gives insight as to *where* the atoms are placed within the structure.

Also, the original yttrium compound has a double-peak at around 33° that is not expressly replicated in the other four compounds. This is likely a result of small differences in cell size and ionic radius, which will be explored later. Overall, however, the peaks are very similar in their locations.

In addition to comparing the graphs of the substituted compounds, the unit cell volumes of each structure can be compared to gain a more direct understanding of how the lattice may have changed. The cell volume of an orthorhombic crystal can be represented by the equation

$$V = abc,$$

where V represents volume and a , b , and c represent the crystal's lattice parameters. The lattice parameters and cell volume of the compounds are represented in Table 5.

Table 5: Lattice Parameters and Cell Volumes of Substituted Compounds

Compound	Ionic Radius * ²⁷	a Value (Å)	b Value (Å)	c Value (Å)	Cell Volume (Å ³)
$\text{YBa}_2\text{Cu}_3\text{O}_{(7-x)}$ Sample 1	1.04 - 1.215	3.815	3.886	11.65	172.7122985
$\text{YBa}_2\text{Cu}_3\text{O}_{(7-x)}$ Sample 2	1.04 - 1.215	3.825	3.89	11.65	173.3432625
$\text{DyBa}_2\text{Cu}_3\text{O}_{(7-x)}$	1.052 - 1.223	3.83	3.883	11.67	173.5549563

$\text{SmBa}_2\text{Cu}_3\text{O}_{(7-x)}$	1.098 - 1.38	3.85	3.91	11.73	176.577555
$\text{NdBa}_2\text{Cu}_3\text{O}_{(7-x)}$	1.123 - 1.41	3.875	3.91	11.73	177.7241625
$(\text{Nd}_{1/3}\text{Sm}_{1/3}\text{Dy}_{1/3})\text{Ba}_2\text{Cu}_3\text{O}_{(7-x)}$	varies	3.85	3.89	11.69	175.075285

* Ionic radius varies depending on coordination within the crystal. Here, the range of possible ionic radii are given, though such values are actually, in fact, discrete.

According to the cell volume calculations, the neodymium compound experienced the most change, expanding to a cell volume of 177.7 \AA^3 , followed by the samarium substituted compound with a cell volume of 176.6 \AA^3 . Neodymium and samarium have the greatest ionic radii of the four metals, and thus took up more space within the unit cell and expanded it. Note, however, that a degree of variation in cell volume exists between the two yttrium samples themselves, and both superconducted. This indicates that superconductivity can be maintained even with slight changes in lattice dimensions. Overall, the compounds maintained similar cell volumes, remaining within $\pm 2\text{-}3\%$ of each other.

2. $\text{YBaCaCu}_3\text{O}_{(7-x)}$

In addition to performing standard yttrium substitutions, one compound had a substitution made of one of the barium ions by replacing it with a calcium ion, giving the formula $\text{YBaCaCu}_3\text{O}_{(7-x)}$. The stoichiometry used to calculate the formation had an error, and so its lattice structure formed differently. (Figure 10).

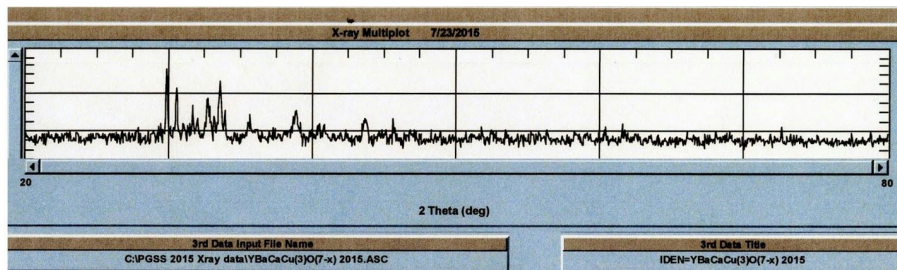


Figure 10: X-ray Diffraction Multiplot of $\text{YBaCaCu}_3\text{O}_{(7-x)}$

Because the structure is so different, its lattice parameters could not be determined using the program which was used for the other compounds. Its cell volume thus remains unknown.

3. Doped Compounds

The doped compounds involved some changes in structure, but not extreme changes (Figures 11 and 12). The crystals are still orthorhombic, and the major peaks from the yttrium compound (at the bottom of Figure 11) are still visible, forming nearly identical x-ray plots.

Of the five doped compounds, the bismuth based one exhibited the greatest differences in peak orientation. At around 29° a major peak is present where no such peak exists in the yttrium compound. While this is a noticeable change, it is not a major one, since the rest of the structure is relatively unaltered and intensity is not a factor. Conversely, the compounds with gallium and silver as dopants have nearly identical peak plots to that of the pure yttrium compound. Gallium and silver are the smallest of the dopants, while bismuth is the largest, which corresponds with the results obtained from x-ray diffraction.

Because the bismuth atoms are larger, they disrupt the original crystal lattice structure more than the other compounds, resulting in more drastic differences in ionic spacing and noticeable changes in diffraction patterns. While gallium and silver maintained a lattice structure more similar to the base compound's, however, this did not necessarily directly correlate with superconductivity. Gallium, for example, lowered the compound's critical temperature, while bismuth raised it slightly.

Though the doped compounds exhibited slightly more variation than the substituted compounds, an interesting similarity exists between the former and the base compounds. Because only a small amount of dopant is added, some form of a double peak at 23° is maintained for all of the doped compounds except for gallium.

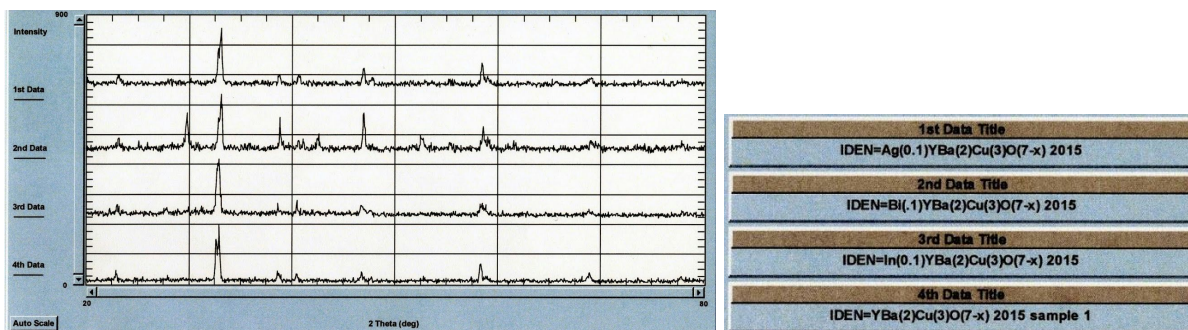


Figure 11: X-ray Diffraction Multiplot of Doped Compounds

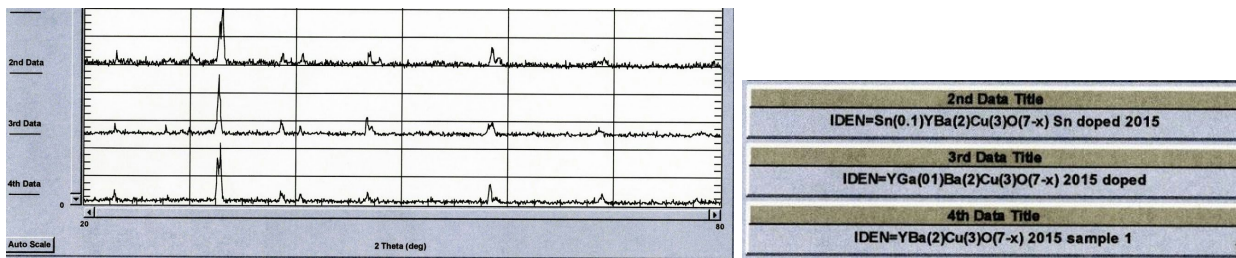


Figure 12: X-ray Diffraction Multiplot of Doped Compounds (sans 1st data plot; not shown)

When the doped compound diffraction plots are compared to the plots of their respective dopants, very little similarities are noticeable (Figures 13 and 14). Likely, this is both a result of the small amount of dopant added, as well as the fact that the dopant ions are oriented differently with respect to other ions in the orthorhombic lattice than when in their pure form. None of the metallic oxides are naturally orthorhombic.

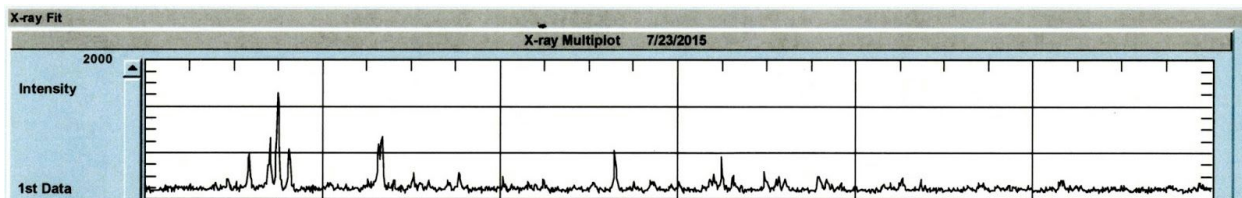


Figure 13: X-ray Diffraction of Bi_2O_3

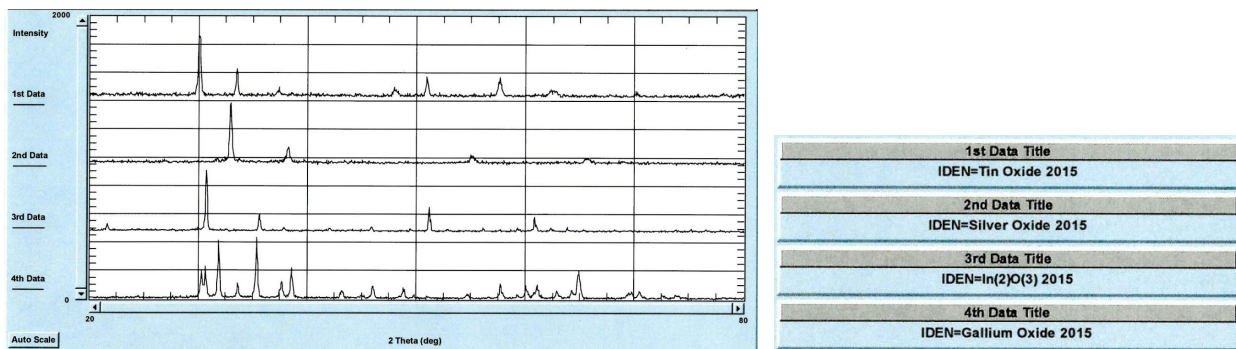


Figure 14: X-ray Diffraction Multiplot of Metallic Oxide Dopants

Compared to the substituted compounds, the doped compounds maintained a cell volume closer to that of the base sample's; all the cell volumes are within $\pm 2\%$ and within $>1\%$ of the base compound's average volume. Like with the peak plots, this is likely a result of the dopant ions being much smaller than most of the surrounding atoms

Table 6: Lattice Parameters and Cell Volumes of Doped Compounds

Compound	Ionic Radius (Å) 27	Charge	a Value (Å)	b Value (Å)	c Value (Å)	Cell Volume (Å³)
YBa ₂ Cu ₃ O _(7-x) Sample 1	-	-	3.815	3.886	11.65	172.7122985
YBa ₂ Cu ₃ O _(7-x) Sample 2	-	-	3.825	3.89	11.65	173.3432625
Sn _(0.1) YBa ₂ Cu ₃ O _(7-x)	0.55 - 0.81	+4	3.8	3.89	11.65	172.2103
Ga _(0.1) YBa ₂ Cu ₃ O _(7-x)	0.61 - 0.76	+3	3.89	3.85	11.65	174.476225
Ag _(0.1) YBa ₂ Cu ₃ O _(7-x)	1.00 - 1.28	+1	3.82	3.89	11.62	172.670876
In _(0.2) YBa ₂ Cu ₃ O _(7-x)	0.76 - 1.06	+3	3.82	3.89	11.62	172.670876
Bi _(0.2) YBa ₂ Cu ₃ O _(7-x)	1.10 - 1.31	+3	3.79	3.89	11.62	171.314822

Bismuth, which resulted in the most disruption of the crystal lattice, also exhibited the greatest deviation from standard cell volume. Interestingly, though, cell volume *decreased* when bismuth was added, though it is among the larger dopants. This does not necessarily mean that the crystal lattice experienced less change, but that it experienced it in a different way. However, in general, cell volume and ionic radius maintain a direct positive correlation (Figure 15). In this case, other factors such as electric properties and electron orbitals likely have an effect.

While dopant charge likely played a role in electron interactions, it does not appear to have been a major factor in lattice structure. Gallium has the same charge as indium, for example, but gallium increased cell volume 0.8%, while indium decreased it by 0.2%. Conversely, tin and silver both achieved virtually identical cell volumes while having different charges. Thus, other electronic characteristics besides charge, such as orbitals and spin, likely contributed to cell volume.

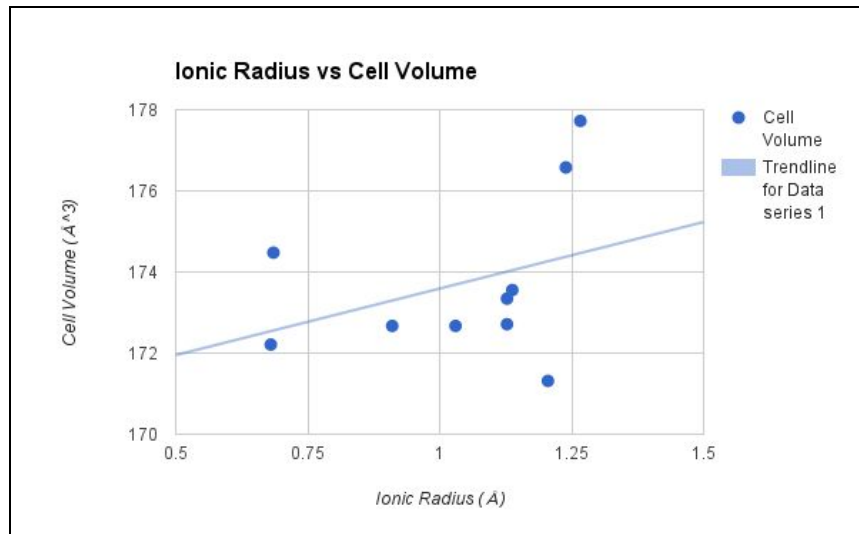


Figure 15: Ionic Radius vs Cell Volume

4. Cell Volume and Critical Temperature

Because lattice structure has an influence on superconductivity, it is necessary to analyze the relationship between the two (Table 7). When the unit cell volume of each of the tested compounds is compared to that compound's superconductivity, a negative correlation is found to exist between the two (Figure 16). Thus, at least for yttrium-based perovskites, a smaller cell volume favors a higher critical temperature. This would explain why bismuth, which resulted in a smaller unit cell when doped, contributed to a more favorable critical temperature than any of the substituted compounds did, all of which increased cell volume. Increasing cell volume likely disrupts the role the oxygen chains play in superconductivity, hindering the electrons' progress of the pair through the lattice. Also, If the volume is wider, the ions are packed less tightly and therefore more susceptible to thermal vibrations, whereas the more closely packed ions are more likely to distribute such vibrations more evenly and mitigate their intensity.

Table 7: Cell Volume and Critical Temperature of Tested Compounds

Compound	Cell Volume (\AA^3)	Critical Temperature (K)
$\text{YBa}_2\text{Cu}_3\text{O}_{(7-x)}$ Sample 1	172.7122985	92.2
$\text{YBa}_2\text{Cu}_3\text{O}_{(7-x)}$ Sample 2	173.3432625	91.9
$\text{DyBa}_2\text{Cu}_3\text{O}_{(7-x)}$	173.5549563	89.9

$\text{SmBa}_2\text{Cu}_3\text{O}_{(7-x)}$	176.577555	91.8
$\text{NdBa}_2\text{Cu}_3\text{O}_{(7-x)}$	177.7241625	-
$(\text{Nd}_{1/3}\text{Sm}_{1/3}\text{Dy}_{1/3})\text{Ba}_2\text{Cu}_3\text{O}_{(7-x)}$	175.075285	-
$\text{Sn}_{(0.1)}\text{YBa}_2\text{Cu}_3\text{O}_{(7-x)}$	172.2103	91.4
$\text{Ga}_{(0.1)}\text{YBa}_2\text{Cu}_3\text{O}_{(7-x)}$	174.476225	86.5
$\text{Ag}_{(0.1)}\text{YBa}_2\text{Cu}_3\text{O}_{(7-x)}$	172.670876	93.6
$\text{In}_{(0.2)}\text{YBa}_2\text{Cu}_3\text{O}_{(7-x)}$	172.670876	-
$\text{Bi}_{(0.2)}\text{YBa}_2\text{Cu}_3\text{O}_{(7-x)}$	171.314822	94.4

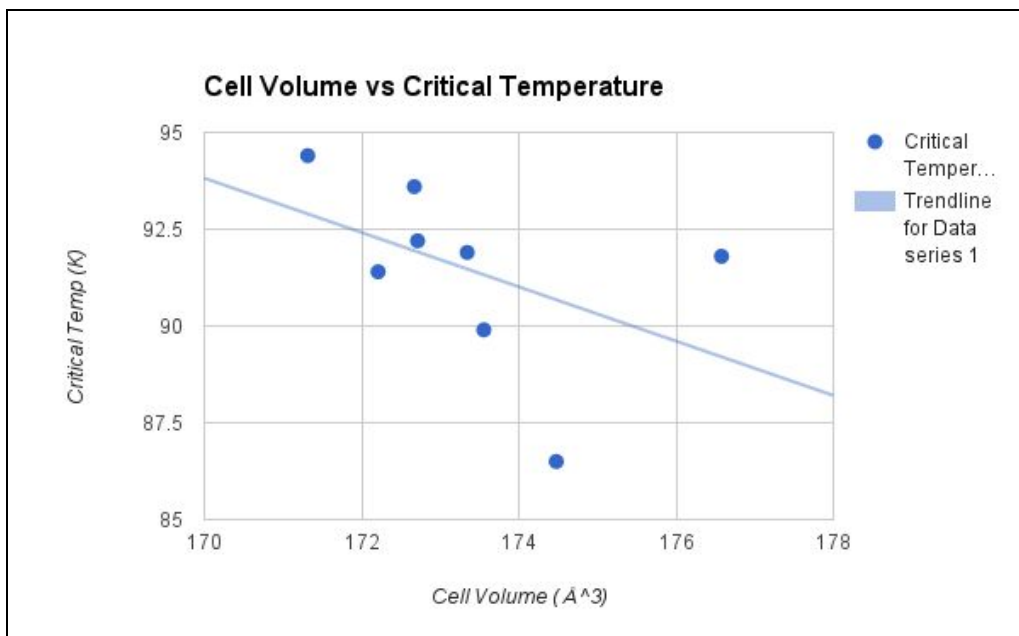


Figure 16: Correlation between Cell Volume and Critical Temperature

It is important to note, though, that exceptions do exist to this model. The samarium substituted compound, for example, had a critical temperature relatively close to yttrium's, but it also had the largest cell volume among the tested samples. Thus, while lattice structure and physical dimensioning are undoubtedly relevant to superconductivity, they are not the only factors contributing to the phenomenon. Further research must be conducted if this is to be better understood.

V. Discussion

A. YBCO Base

1. $\text{YBa}_2\text{Cu}_3\text{O}_{(7-x)}$ (Sample 1)

The standard 1-2-3 YBCO ($\text{YBa}_2\text{Cu}_3\text{O}_{(7-x)}$) base superconducted with a T_c of 92.2 K (Figure 14). This was very close to the T_c of industrially created and tested YBCO base, which is 92K (percent error = -0.217%). The successful creation of a good standard base evidenced the fact that functioning superconductors could be created through this method; thus, substitution and doping could be carried out.

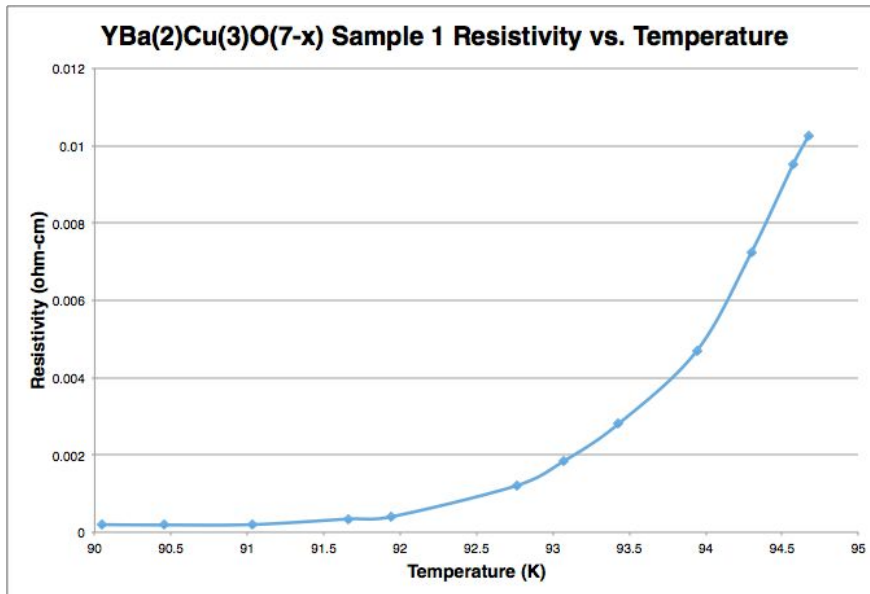


Figure 17: Sample 1 $\text{YBa}_2\text{Cu}_3\text{O}_{(7-x)}$ Resistivity vs Temperature

2. $\text{YBa}_2\text{Cu}_3\text{O}_{(7-x)}$ (Sample 2)

The standard YBCO base superconducted with a T_c of 91.9 K (Figure 15). This was very close to the T_c of industrially created and tested YBCO base, which is 92K (percent error = 0.109%). The repeated success in creating the YBCO base was a promising sign regarding the ability to create superconducting samples correctly.

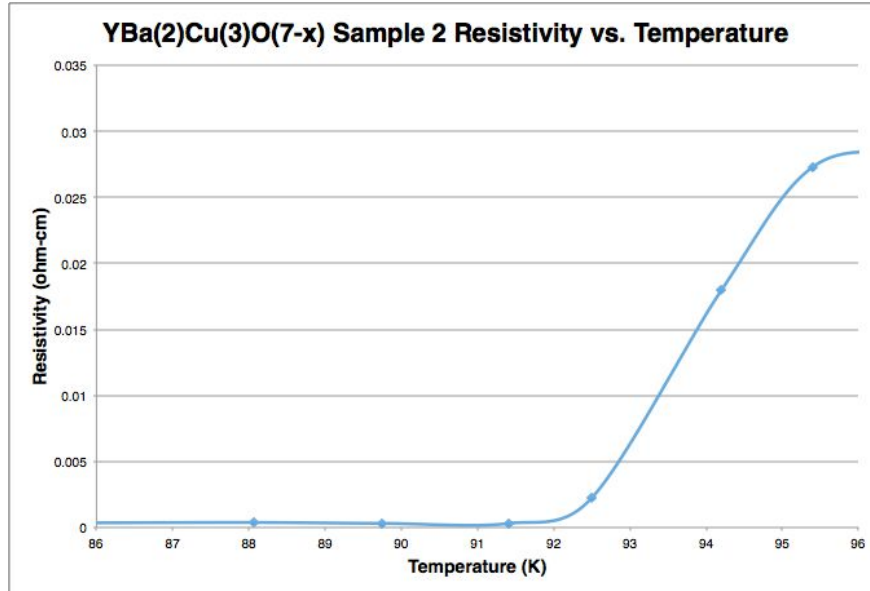


Figure 18: Sample 2 $\text{YBa}_2\text{Cu}_3\text{O}_{(7-x)}$ Resistivity vs Temperature

B. Substituted Samples

$\text{DyBa}_2\text{Cu}_3\text{O}_{(7-x)}$

The dysprosium-substituted sample successfully superconducted with a T_c of 89.9 K (Figure 16). This was slightly lower than the critical temperature of the YBCO base compound, meaning the substitution lowered the superconducting abilities of the base compound.

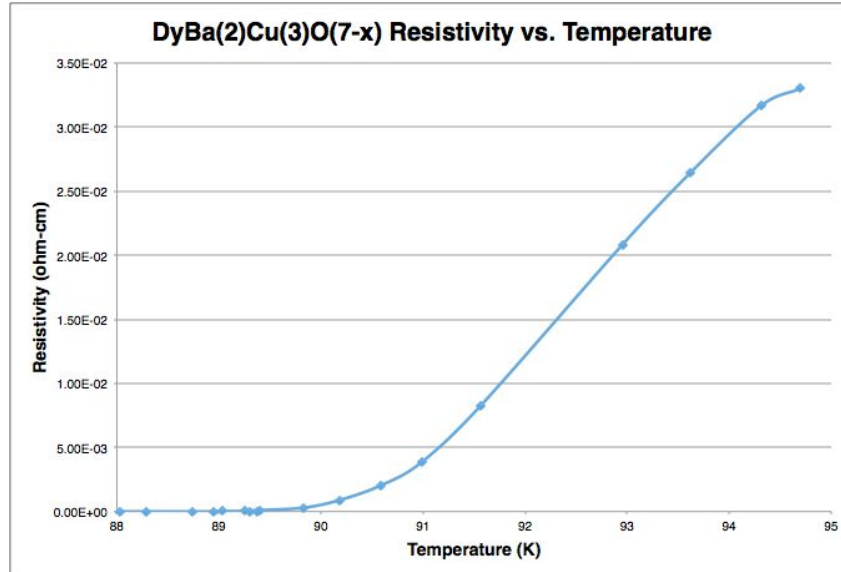


Figure 19: $\text{DyBa}_2\text{Cu}_3\text{O}_{(7-x)}$ Resistivity vs Temperature

2. $\text{SmBa}_2\text{Cu}_3\text{O}_{(7-x)}$

The samarium-substituted sample successfully superconducted with a T_c of 91.8 K (Figure 17), or barely lower than the YBCO base, meaning that the substitution very slightly lowered the superconducting abilities of the base compound.

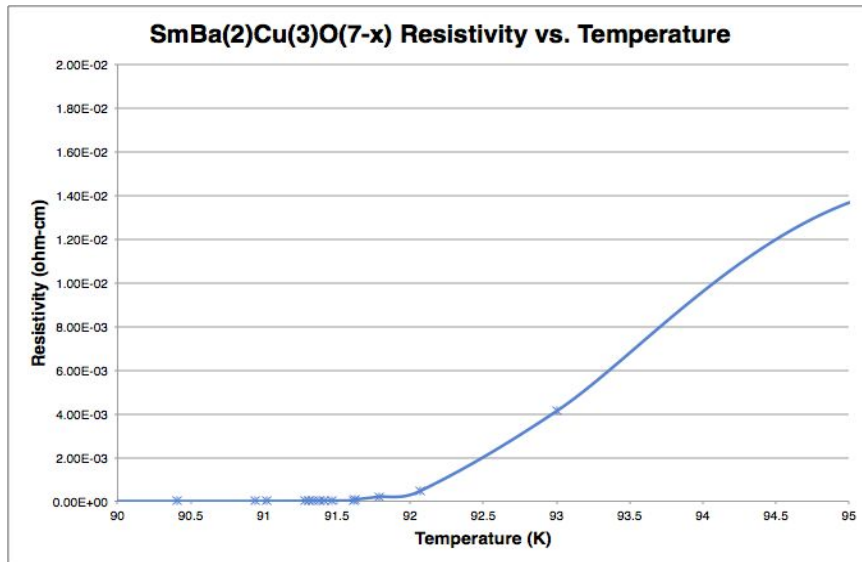


Figure 20: $\text{SmBa}_2\text{Cu}_3\text{O}_{(7-x)}$ Resistivity vs Temperature

3. $\text{NdBa}_2\text{Cu}_3\text{O}_{(7-x)}$

The neodymium substituted sample potentially might superconduct at lower temperatures, based on the fact that the graph's shape has similarities to the graphs of conclusively superconducting samples (Figure 18). However, the exact temperature cannot be determined by the data collected because the liquid nitrogen used to cool the sample to determine resistivity was not cold enough to accurately measure such low temperatures.

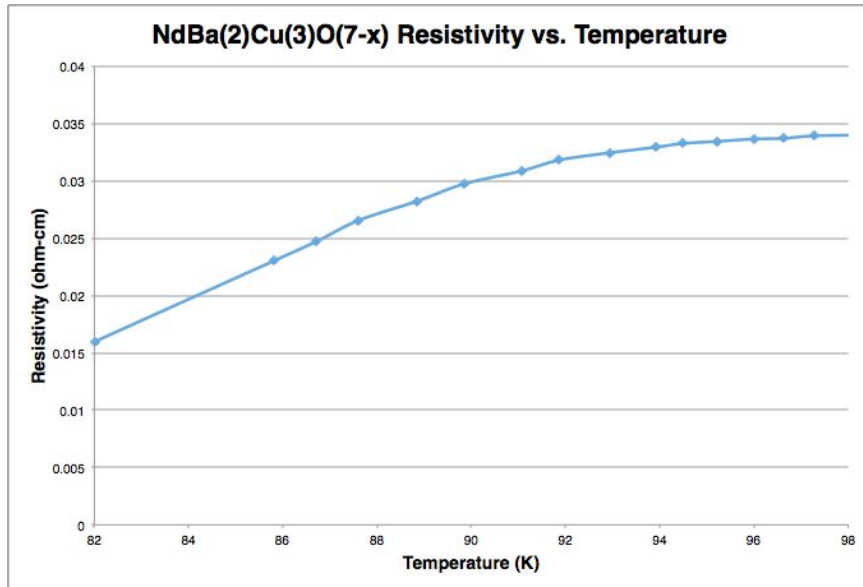


Figure 21: $\text{NdBa}_2\text{Cu}_3\text{O}_{(7-x)}$ Resistivity vs Temperature

4. $\text{YBaCaCu}_3\text{O}_{(7-x)}$

The sample of YBCO with some calcium substituted for barium also could superconduct at lower temperatures (Figure 19). Once again, however, the exact temperature cannot be determined by the data collected because the liquid nitrogen used to cool the sample to determine resistivity was not cold enough to accurately measure such low temperatures. Because the amount of barium oxide available was all used up, a barium calcium copper oxide was tested to see if the sample would superconduct.

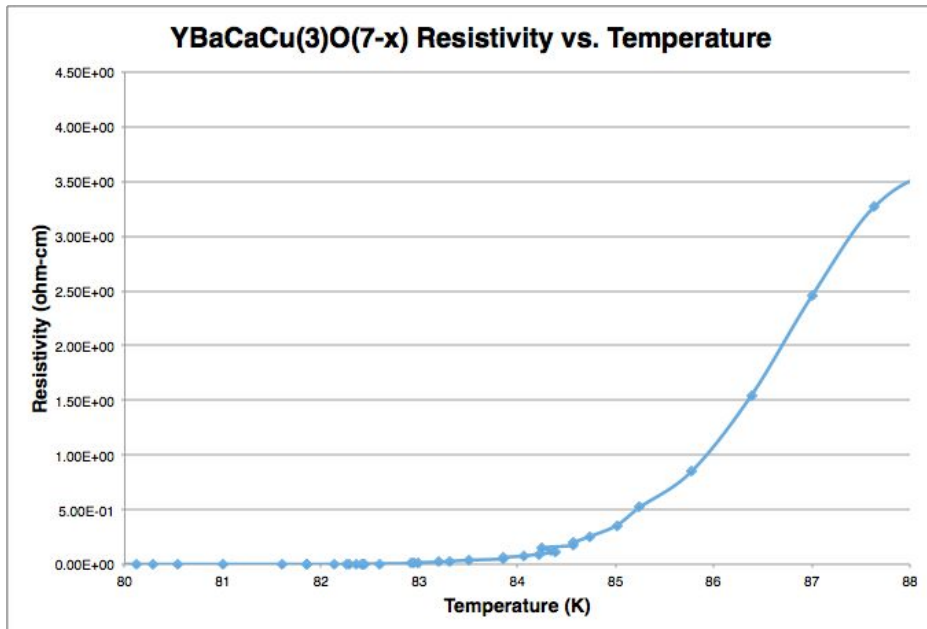


Figure 22: $\text{YBaCaCu}_3\text{O}_{(7-x)}$ Resistivity vs Temperature

5. $(Nd_{1/3}Sm_{1/3}Dy_{1/3})Ba_2Cu_3O_{(7-x)}$

Although full substitutions of all three elements did superconduct to varying extents (Figure 20), a partial substitution with the three substituted for yttrium in equal amounts does not superconduct. This could have been because of the varying sizes of the three substituent elements. For full substitutions, all the atoms in the crystal lattice area for yttrium are the same size and chemical, thus the crystal lattice is homogenous and uniform. When multiple different elements are substituted in, it is possible to get a nonuniform crystal lattice, interfering with superconductivity.

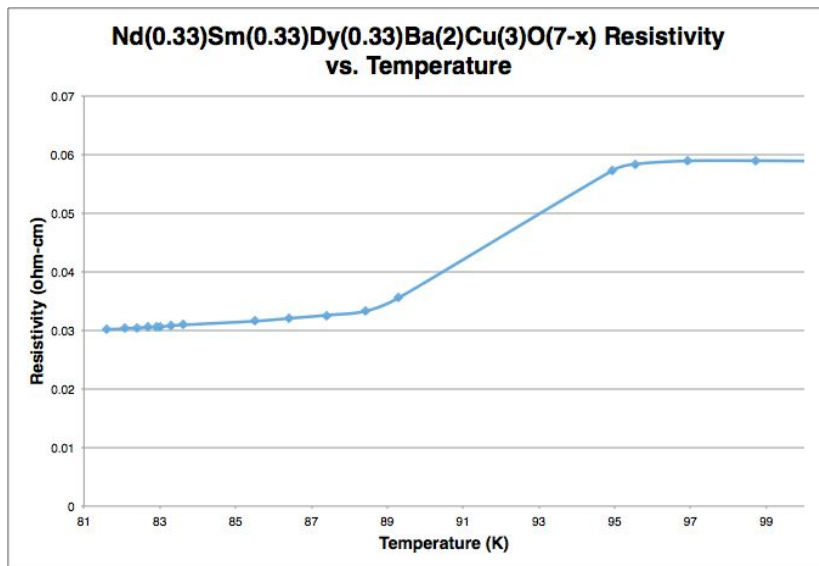


Figure 23: $(Nd_{1/3}Sm_{1/3}Dy_{1/3})Ba_2Cu_3O_{(7-x)}$ Resistivity vs Temperature

C. Doped Compounds

1. $In_{(0.2)}YBa_2Cu_3O_{(7-x)}$

The sample with 20% by mole indium doped in potentially could superconduct at lower temperatures (Figure 21); however, similar to the full neodymium substitution and the partial calcium substitution, it superconducts at temperatures too low to accurately measure with the liquid nitrogen coolant.

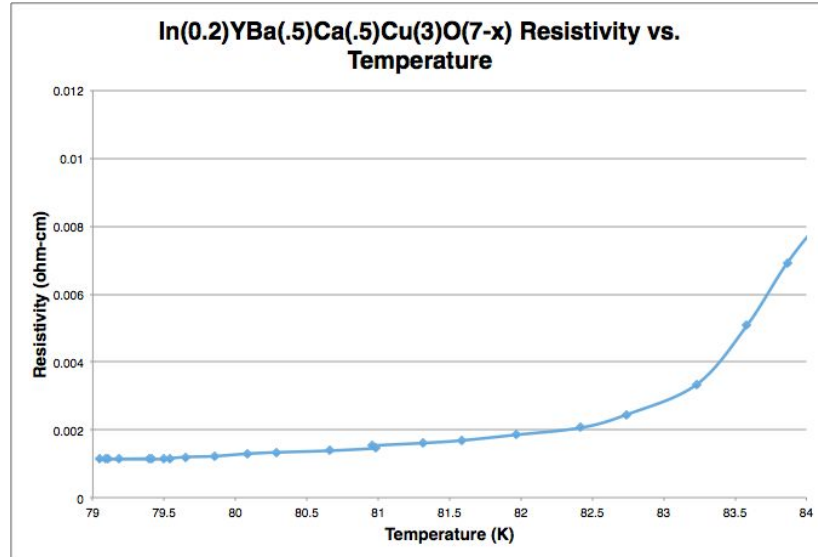


Figure 24: In_(0.2)YBa₂Cu₃O_(7-x) Resistivity vs Temperature

2. Ag_(0.1)YBa₂Cu₃O_(7-x)

The sample with 10% by mole silver doped superconducts at a T_c of 93.6 K (Figure 22), or 1.11% higher than the YBCO base. This was a successful trial in which the YBCO base superconductor was actually improved by raising the T_c.

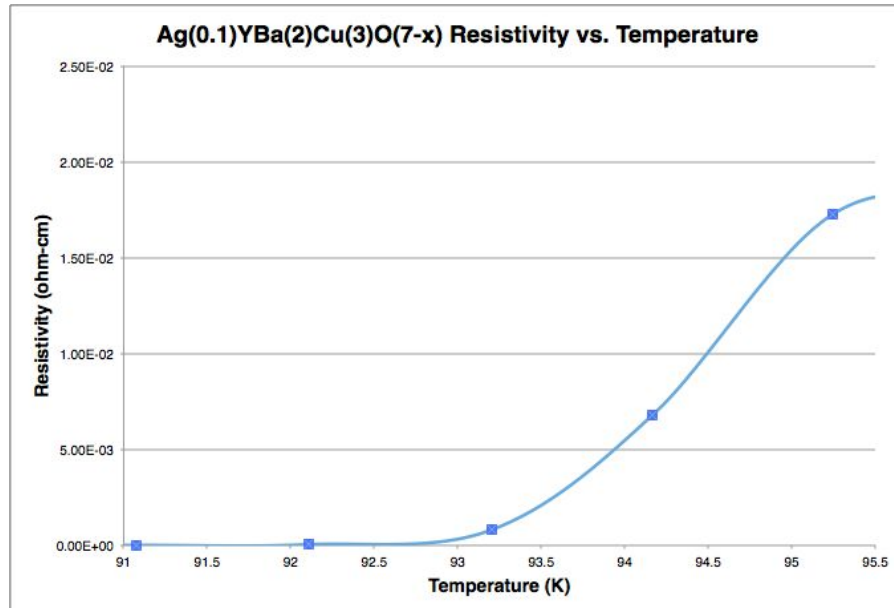


Figure 25: Ag_(0.1)YBa₂Cu₃O_(7-x) Resistivity vs Temperature

3. Bi_(0.2)YBa₂Cu₃O_(7-x)

The sample with 20% by mole bismuth doped superconducts at a T_c of 94.4 K (Figure 23), or 2.61% higher than the YBCO base. This was a successful trial in which the YBCO base superconductor was actually improved by raising the T_c quite significantly (even more so than the silver dopant).

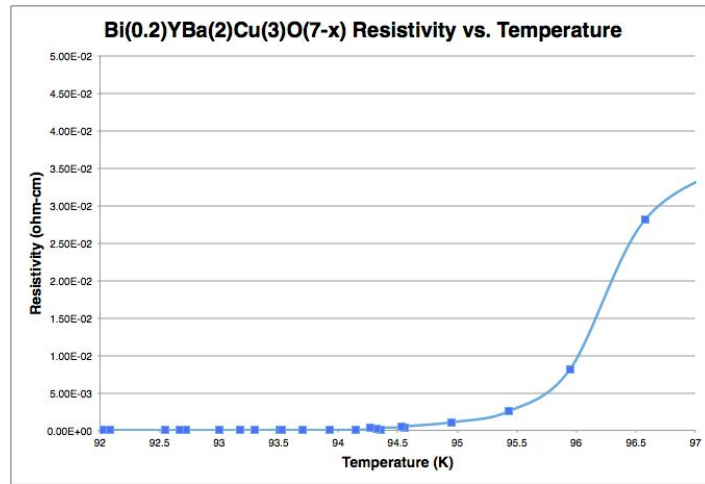


Figure 26: $\text{Bi}_{(0.2)}\text{YBa}_2\text{Cu}_3\text{O}_{(7-x)}$ Resistivity vs Temperature

4. $\text{Ga}_{(0.1)}\text{YBa}_2\text{Cu}_3\text{O}_{(7-x)}$

The sample with 10% by mole gallium doped superconducts at a T_c of 86.5 K (Figure 24), quite a bit lower than the YBCO base. The addition of a gallium dopant lowered the superconductivity of the YBCO base significantly.

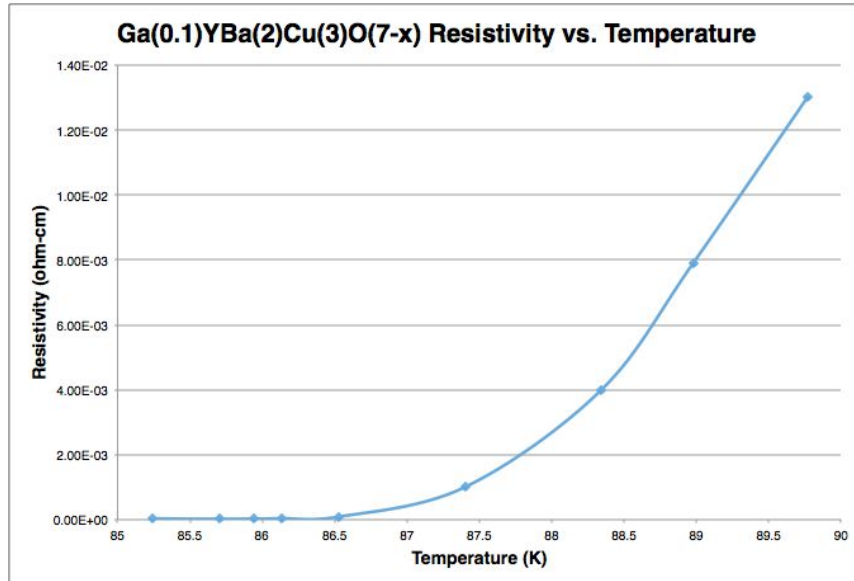


Figure 27: $\text{Ga}_{(0.1)}\text{YBa}_2\text{Cu}_3\text{O}_{(7-x)}$ Resistivity vs Temperature

5. $\text{Sn}_{(0.1)}\text{YBa}_2\text{Cu}_3\text{O}_{(7-x)}$

The sample with 10% by mole tin doped superconducts at a T_c of 91.4 K, slightly lower than the YBCO base. The addition of a tin dopant lowered the superconductivity of the YBCO base.

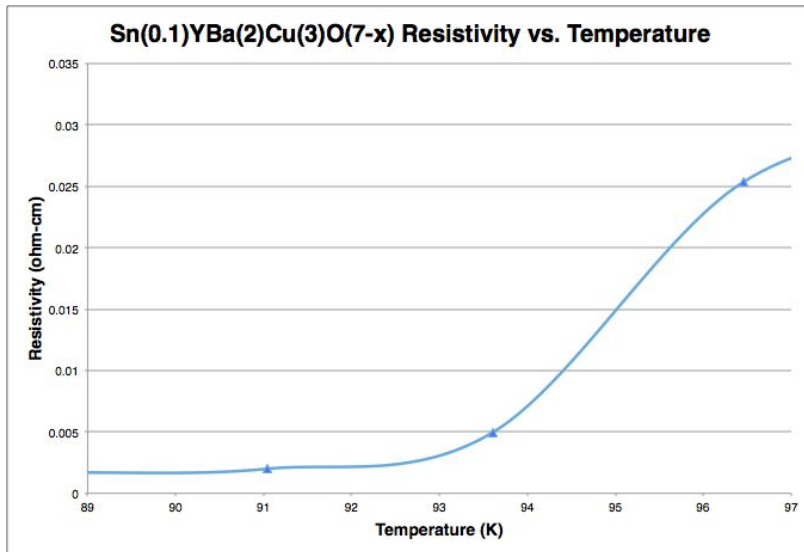


Figure 28: $\text{Sn}_{(0.1)}\text{YBa}_2\text{Cu}_3\text{O}_{(7-x)}$ Resistivity vs Temperature

C. Analysis of Critical Current Density Graph

Using the above graphs, T_c values were calculated by finding the point on the graph at which the tangent is sharply increases. These values are then plotted against the critical current density (Figure 26), which is found by first finding the current using Ohm's Law since voltage and resistance are both known and then dividing that value by the cross-sectional area of the sample, i.e. width \times height. The graphs can be analyzed by their lines of best fit (Figure 27). The goal of this experiment was to find a superconductor with a higher T_c than the currently available YBCO samples. Thus, the graph with an x-intercept that is most shifted to the right has a higher such temperature and was more successful.

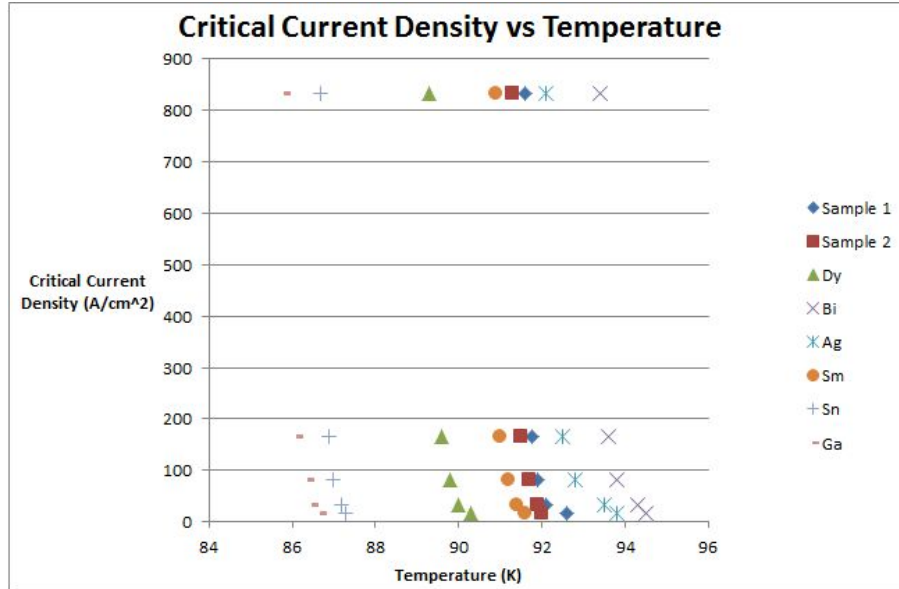


Figure 29: Critical Current Density vs Temperature

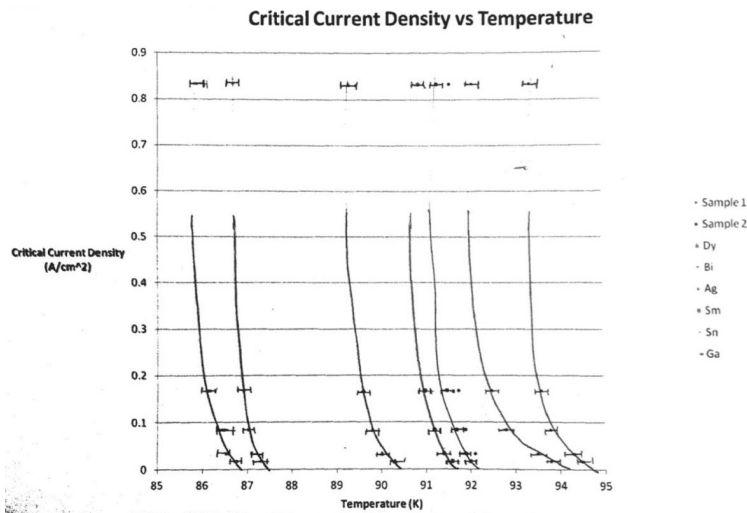


Figure 30: Critical Current Density vs Temperature (Trend Lines)

The error bars above were calculated by determining the shift in temperature between sample 1 and sample 2. This change in temperature is caused by the position of the ice in the dewar. In Figure 30, the line that is third from the right shows the original sample without any dopings or substitutions. According to the above graph, since silver and bismuth are shifted to the right of Sample 1 and/or sample 2, they have higher critical temperatures and therefore were better superconductors. The T_c values were increased almost two degrees. On the other hand, samples such gallium and tin performed poorly, almost decreasing the critical temperature by several degrees.

D. Calculations Related to Electron-Phonon Collisions

Phonon scattering is a scattering of electrons from the interaction with the lattice structure. Using the assumption that electron-phonon collisions are elastic, the mean collision time, denoted by τ can be calculated using the following equation:

$$\tau = m/(ne^2 \sigma T)$$

where m stands for the mass of an electron, n stands for the number of electrons per unit volume (obtained through the calculated lattice parameters), σ stands a temperature dependent resistivity and T stands for the temperature in Kelvin. One can assume that each copper in the crystal structure contributes one electron, meaning that the total number of electrons used in the samples was 3. Using this equation, temperature v. mean collision time was graphed below. Because these values are extremely small, only three lines for sample 1, 2 and dysprosium were graphed so that they can remain distinct (Figure 28). The values indicate clearly that as the temperature increases, the mean collision time decreases, which is consistent with the ideas of vibration in molecules.

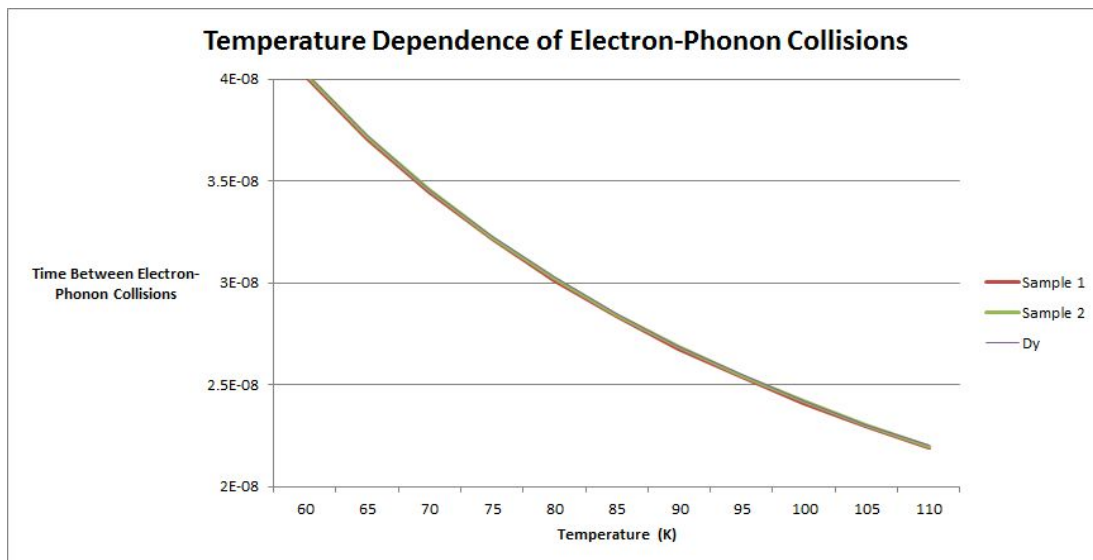


Figure 31: Temperature Dependence of Electron-Phonon Collisions

VI. Conclusion

A. Summary

1. Trends in Yttrium Substitutions

In regards to substitution, all of the full substitutions superconducted at lower temperatures than the YBCO base and the partial .33 substitution did not superconduct. This could potentially be explained by the slight differences in atomic radius and electron distribution between yttrium and the three substitution elements used (dysprosium, neodymium, and samarium). When slightly different elements are substituted into the

base in place of the yttrium, the atom could distort the crystal lattice structure around it, changing the local electronic structure. This change in structure would be small and local because the atomic radii were close but not exactly the same and the elements that were substituted all had electrons in the 4f orbitals, unlike yttrium; thus, the entire crystal structure would not be destroyed, there would be slight local changes in electron density. This slight change in local structure can be seen when analyzing the cell volumes for each sample. The full substitutions of dysprosium and samarium created slightly larger cell volumes than yttrium while the full substitution of neodymium resulted in a much larger cell volume; both dysprosium and samarium samples superconducted at fairly high temperatures while the neodymium sample conducted at a much lower temperature. Both dysprosium and samarium had larger atomic radii than yttrium, and had slightly lower T_c s; neodymium had a smaller atomic radius and has a much lower T_c . If more data points with different substitutions had been taken, it might have been possible to graph atomic radii vs. T_c in order to study in greater detail the effect that size has on superconductivity. Although the crystal lattice may not be changed, this change in electron density could potentially be significant in terms of Cooper pairing interactions and the energy needed to break up the Cooper pairs, leading to a lower energy needed to break up the electron interactions. This would lower superconductivity, but not make the material not superconduct at all.²⁸ The partial substitutions with .33 of each element could have potentially not worked because of differences in the elements substituted. When up to four heavy rare earth metals are substituted in, the samples superconduct and all the critical temperatures are around the parents compound (YBCO base); however, neodymium and samarium are light rare earth metals, meaning they have unpaired electrons in the 4f orbital.³³ This difference in electronic configuration could be the reason behind the lack of superconductivity; however, further research has to be done to figure out conclusively if and why the lack of paired electrons can so drastically affect superconductivity.

2. Trends in Doping

Only the bismuth and silver-doped compounds were successful in superconducting above the critical temperature of the base compound. An important consideration when drawing conclusions from the varying degrees of success of the dopants is ionic radius. As stated above in Table 2, bismuth and silver, the most successful dopants, have similar ionic radii, with silver's being 1.00 - 1.28 Å and bismuth's being 1.10 - 1.31 Å. These atomic radii are significantly larger than the radii of the other dopants, again, as shown in Table 2. All of the dopants were small enough to enter into the crystal lattice and were able to form superconductors (though not all at higher temperatures than the base). A potential reason for bismuth's and silver's effectiveness is some kind of optimal radius for doping of this particular base compound, with its particular lattice structure and base cell size. Bismuth was more effective than silver, possibly because of this kind of optimal radius or because twice as many moles of bismuth were doped in than moles of silver.

Regarding the other compounds, it is possible to analyze electrostatic properties of the doped elements. Gallium and indium, which brought the critical temperature down significantly, have similar electronic structure, with the same number of valence electrons, as they are in the same group on the periodic table. It is possible that their electrostatic properties disrupted the crystal lattice in the same way. Both had a relatively small ionic radius, with indium's being 0.76-1.06 Å and gallium's being 0.61 - 0.76 Å. Indium could have disrupted the lattice and current flow more due to the fact that twice as many moles of indium as gallium was doped in. Tin brought the critical temperature of the base down slightly; it has a similar electron configuration and a slightly smaller size when compared to indium, but has 2 p electrons in its valence shell which is slightly more stable than the ionic form of Indium and Gallium. This could have disrupted the crystal lattice less, but still distorted it slightly.

Without further trials, either with the dopants which were tried or with other elements, it is not possible to conclusively determine a trend for the effectiveness of dopants. Because only one sample was made with each dopant, it is not possible to currently account for slight differences in doping or compound configurations as would be possible with multiple samples. And without samples of more elements, it is not possible to conclusively determine an overall trend across various elements, comparing their properties with their compounds' critical temperatures.

3. Crystal Structure

Plots of intensity peaks were obtained through x-ray diffraction and were used to compare the structures of the doped and substituted compounds to the base yttrium compound. Based on these results, it was found that though both doping and substitution affected lattice structure, it was not to a major degree. Most compounds exhibited little variance with respect to the yttrium compound, with the samarium and neodymium substituted, and bismuth doped compounds deviating the most. These differences related mostly with the ionic radii of the substitute and dopant atoms; the larger the atoms were, the more they warped the crystal lattice and increased cell volume. Additionally, smaller cell volumes were found to be more optimal for higher critical temperatures. Presumably, an increase in cell volume leads to the unit cells expanding. When multiple unit cells expand into the same space, their structures are then warped and disrupted, thereby increasing disorder, making the structure more susceptible to thermal vibrations, and hindering the formation and progress of electrons in the lattice. A smaller cell volume therefore minimizes these effects, and maximizes the conditions necessary for superconductivity. However, exceptions do exist in the data; other variables, such as electronic structure, orbitals, and ionic charge, are likely to have an effect along with physical structure. Thus, silver and bismuth possess the best combination of these characteristics as dopants, while none of the substitutes optimize the characteristics of yttrium.

B. Sources of Error

There are several errors in this experiment. Some of the samples had difficulty making contact with the silver contacts and therefore some of the points on the graph did not follow the trendline exactly. Another error that could have occurred was the imprecise temperature reading of the thermocouple in the ice-water bath. The ice tended to float in the bath instead of being packed at the bottom, which would have been optimal in terms of temperature measurements. Other errors include instrumental error, including the imprecision of the instruments used as well as human error.

C. Further Considerations

There are several further projects that could be done to further explore some of the anomalies that occurred in the data. First, the sample with the calcium could be tried again in an attempt to replicate the results. Another further experiment could be to explore heavier vs lighter rare earth metals. From the experimentation conducted in this project, it appears that the lighter metals do not function as effectively. However, more samples would be needed to better this hypothesis. If more data points with different substitutions had been taken, it might have been possible to graph atomic radii vs. T_c in order to study in greater detail the effect that size has on superconductivity. From the current data, further experimentation

should involve smaller cell sizes in terms of lattice parameters. Another possible experiment would be use liquid helium, which is much colder than liquid nitrogen.

Acknowledgements

This project would not have been possible without the guidance of our advisor and mentor Dr. Richard Butera, teaching assistants Aria Soltani and David Vinson, fellow classmates, supportive parents, and the PGSS faculty and staff, including Program Director Dr. Barry Luokkala.

Additionally, this program would not have been possible without the sponsorship of the Pennsylvania Department of Education and the support of the Team Pennsylvania Foundation, the PGSS Campaign and generous alumni, and our corporate donors: EQT, TEVA Pharmaceuticals, AT&T, PPG, and the Grable Foundation, who allowed us to have this opportunity. Further thanks goes to Carnegie Mellon University and its faculty and staff, who allowed us to use their equipment and facilities throughout the duration of the program.

Appendix A: Stoichiometric Calculations

Base Compound: Calculated how many moles of the base compound were needed to make a five gram sample and used this value to calculate the mass of each oxide needed to make the base compound.

$$\begin{aligned} 5.0 \text{ g } \text{TBa}_2\text{Cu}_3\text{O}_{7-x} &\div 666.0 \text{ g/mol} = 0.00750 \text{ mol } \text{YBa}_2\text{Cu}_3\text{O}_{7-x} \\ 0.00750 \text{ mol } \text{YBa}_2\text{Cu}_3\text{O}_{7-x} \times (2 \text{ Ba}) \times (1 \text{ BaO}) \times 153.5 \text{ g} &= 2.30 \text{ g BaO} \\ 0.00750 \text{ mol } \text{YBa}_2\text{Cu}_3\text{O}_{7-x} \times (3 \text{ Cu}) \times (1 \text{ CuO}) \times 79.5 \text{ g} &= 1.79 \text{ g CuO} \\ 0.00750 \text{ mol } \text{YBa}_2\text{Cu}_3\text{O}_{7-x} \times (1 \text{ Y}) \div (2 \text{ Y}) \times (225.8 \text{ g}) &= 0.847 \text{ g Y2O3} \end{aligned}$$

Substitutions: Used the moles of yttrium needed to convert to moles of the element being substituted and then converted that to the moles of the oxide and finally to the grams of that oxide needed.

$$\begin{aligned} \text{Dysprosium} - 0.00750 \text{ mol } \text{YBa}_2\text{Cu}_3\text{O}_{7-x} \div (2 \text{ Dy}) \times (373.0 \text{ g}) &= 1.40 \text{ g Dy2O3} \\ \text{Neodymium} - 0.00750 \text{ mol } \text{YBa}_2\text{Cu}_3\text{O}_{7-x} \div (2 \text{ Nd}) \times (336.5 \text{ g}) &= 1.26 \text{ g Nd2O3} \\ \text{Samarium} - 0.00750 \text{ mol } \text{YBa}_2\text{Cu}_3\text{O}_{7-x} \div (2 \text{ Sm}) \times (348.8 \text{ g}) &= 1.31 \text{ g Sn2O3} \end{aligned}$$

Partial Substitution: Because elements were substituted in for yttrium, the number of moles of yttrium needed in the base compound was multiplied by $\frac{1}{3}$ to get the number of moles of each substitute was needed. That value was then converted into grams of the oxides needed to make the partial substitution.

$$\begin{aligned} 0.00750 \text{ mol } \text{YBa}_2\text{Cu}_3\text{O}_{7-x} \times (1/3) \times (336.4 \text{ g}) &= 0.841 \text{ g Nd2O3} \\ 0.00750 \text{ mol } \text{YBa}_2\text{Cu}_3\text{O}_{7-x} \times (1/3) \times (348.8 \text{ g}) &= 0.872 \text{ g Sm2O3} \\ 0.00750 \text{ mol } \text{YBa}_2\text{Cu}_3\text{O}_{7-x} \times (1/3) \times (373.0 \text{ g}) &= 0.933 \text{ g Dy2O3} \end{aligned}$$

$\text{YBaCaCu}_3\text{O}_7$ Compound (0.00879 mol):

First the amount of yttrium needed was calculated.

$$0.00879 \text{ mol Y} \div (2 \text{ Y}) \times (225.81 \text{ g}) = 0.9924 \text{ g Y2O3}$$

Because all the barium oxide was used up, a barium calcium copper oxide compound was used in its place. The amount of barium needed was calculated and then the amount of this mixed compound needed was calculated as well.

$$0.00477 \text{ mol Ba} \div (2 \text{ Ba}) \times (521.829 \text{ g}) = 1.2446 \text{ g Ba2CaCu2O3}$$

Because there is some copper included in the previous compound, the amount of copper needed was decreased by the amount of copper included in the previous compound, and the remaining amount of copper needed was calculated and then the amount of copper oxide needed to provide that amount of copper was calculated.

$$0.01557 \text{ mol Cu} \times 79.5454 \text{ g} = 1.239 \text{ g CuO}$$

Doping: For the first four dopants 10% of the total number of moles was added, and this value was then converted to moles of each particular oxide. For the last two dopants 20% of the total number of moles was added and then converted to grams of the oxide.

$$\begin{aligned} \text{Silver} - 0.000750 \text{ mol Ag} \div (2 \text{ Ag}) \times (231.8 \text{ g}) &= .0869 \text{ g Ag2O} \\ \text{Indium} - 0.000750 \text{ mol In} \div (2 \text{ In}) \times (277.6 \text{ g}) &= 0.104 \text{ g In2O3} \\ \text{Tin} - 0.000750 \text{ mol Sn} \times (134.7 \text{ g}) &= 0.101 \text{ g SnO} \\ \text{Gallium} - 0.00750 \text{ mol Ga} \div (2 \text{ Ga}) \times (187.4 \text{ g}) &= 0.0703 \text{ g Ga2O3} \end{aligned}$$

Indium - 0.0015 mol In $\div (2 \text{ In}) \times (277.6 \text{ g}) = 0.208 \text{ g In}_2\text{O}_3$

Bismuth: - 0.0015 mol Bi $\div (2 \text{ Bi}) \times (466.0 \text{ g}) = 0.350 \text{ g Bi}_2\text{O}_3$

References

1. The History of Superconductors [The History of Superconductors]. (n.d.). Retrieved July 27, 2015, from superconductors.org website: <http://www.superconductors.org/history.html>
2. The effect of oxygen doping on the superconductivity of $\text{Bi}_2\text{CaSr}_2\text{Cu}_2\text{O}_{8-\delta}$. (n.d.). Retrieved July 27, 2015, from <http://www.sciencedirect.com/science/article/pii/092145349191643I?np=y>
3. "Superconductivity: Present and Future Applications." (2008): n. pag. Ccas-web.org. IEEE, Coalition for the Commercial Application of Superconductors, 2009. Web. 27 July 2015, from http://www.ccas-web.org/pdf/ccas_brochure_web.pdf
4. Amin, S. Massoud. "U.S. Electrical Grid Gets Less Reliable." *Spectrum.ieee.org*. IEEE, 24 Jan. 2011. Web. 27 July 2015, from <http://spectrum.ieee.org/energy/policy/us-electrical-grid-gets-less-reliable>
5. Yoshida, Reiji. Japanese maglev train. Digital image. *Japantimes.co.jp*. Japan Times, 30 Sept. 2013. Web. 27 July 2015, from <http://www.japantimes.co.jp/news/2013/09/30/reference/maglev-challenge-both-technical-financial/>
6. Aarnink, René, and Johan Overweg. "Magnetic Resonance Imaging, a Success Story for Superconductivity." *Europhysics News* 43.4 (2012): 26-29. *Europhysicsnews.org*. Europhysics News, 2012. Web. 27 July 2015, from <http://www.europhysicsnews.org/articles/epn/pdf/2012/04/epn2012434p26.pdf>
7. Buchler, Ben. Cooper Pairs. Digital image. *ABC Science*. N.p., 20 July 2011. Web. 29 July 2015, from http://webs.mn.catholic.edu.au/physics/emery/hsc_ideasImplementation.htm
8. Barry, T. (n.d.). BCS Theory of Superconductivity. Retrieved July 23, 2015, from http://ffden-2.phys.uaf.edu/212_fall2003.web.dir/t.j_barry/bcstheory.htmlc
9. Bardeen, J., Cooper, L., & Schrieffer, J. (1957). PhysRev.108.1175. Phys. Rev, 108(5), 1175-1204. doi:10.1103/PhysRev.1081175
10. Saxena, A. (n.d.). Crystal Structure of High Temperature Superconductors. In *High-Temperature Superconductors* (pp. 43-46). Springer Science & Business Media.
11. Withers, N. (n.d.). YBCO - Yttrium Barium Copper Oxide. Retrieved from Royal Society of Chemistry: Chemistry World website: <http://www.rsc.org/chemistryworld/2013/05/yttrium-barium-copper-oxide-ybcos-podcast>
12. Saxena, A. K. (n.d.). Crystal structure of high temperature superconductors. In *High temperature superconductors* (pp. 43-45). Springer Science & Business Media.

13. "Insulators, Conductors, Semiconductors, and Superconductors." *PBS*. PBS, ScienCentral Inc, The American Institute of Physics, 1999. Web. 27 July 2015, from <http://www.pbs.org/transistor/science/info/conductors.html>
14. Zumdahl, Steven S., and Susan A. Zumdahl. "An Introduction to Structures and Types of Solids." *Chemistry*. 9th ed. Belmont: Brooks Cole, 2014. 460-63. Print.
15. "X-ray Basics." *MRL UCSB*. UC Santa Barbara Materials Research Laboratory, 2014. Web. 27 July 2015, from <http://www.mrl.ucsb.edu/centralfacilities/x-ray/basics>
16. xxx Superconductivity. (n.d.). Retrieved from Georgia State University: Hyperphysics website: <http://hyperphysics.phy-astr.gsu.edu/hbase/solids/scond.html>
17. Resistance. (n.d.). Retrieved from Georgia State University: Hyperphysics website: <http://hyperphysics.phy-astr.gsu.edu/hbase/electric/resis.html>
18. Mohs hardness | mineralogy. (n.d.). Retrieved July 23, 2015, from <http://www.britannica.com/science/Mohs-hardness>
19. Wolten, G. M., and A. B. Chase. *Determination of the Point Group of β -Ga₂O₃ from Morphology and Physical Properties*. *ScienceDirect*. Journal of Solid State Chemistry, 15 Jan. 1976. Web. 27 July 2015, from <http://www.sciencedirect.com/science/article/pii/0022459676900542>
20. Rajalingam, Sankeerth. *Theoretical Investigations of β -Ga₂O₃, β -Ga₂Se₃ and β -Ga₂Te₃ Using Ab-initio Calculations*. Utdr.utoledo.edu. The University of Toledo, May 2012. Web. 27 July 2015, from <http://utdr.utoledo.edu/cgi/viewcontent.cgi?article=1432&context=theses-dissertations>
21. Meyer, M., G. Onida, A. Ponchel, and L. Reining. *Electronic Structure of Stannous Oxide*. Wfu.edu. Elsevier, 1998. Web. 27 July 2015, from <http://users.wfu.edu/natalie/s11phy752/lecturenote/Casestudies/SnO.1998.sdarticle-2.pdf>
22. D500 Diffractometer. Digital image. CMMP X-ray Diffraction, 17 June 2011. Web. 26 July 2015, from <http://xrd-cmmp.blogspot.com/2011/06/siemens-d500-powder-diffractometers.html>
23. Screenshot of x-ray scanning program. Digital image. Ksanalytical.com. KS Analytical Systems, n.d. Web. 26 July 2015. <<http://ksanalytical.com/wp-content/uploads/2015/04/VXD.jpg>>.
24. Marezio, M. *Refinement of the Crystal Structure of In₂O₃ at Two Wavelengths*. Acta Crystallographica, 1966. Web. 27 July 2015, form <http://scripts.iucr.org/cgi-bin/paper?a05121>
25. Madelung, O., U. Rossler, and M. Schulz. *Non-Tetrahedrally Bonded Elements and Binary Compounds I: Silver oxides (Ag(x)O(y)) crystal structure, lattice parameters*. Springer Berlin Heidelberg, 1998. Web. 27 July 2015, from http://link.springer.com/chapter/10.1007/10681727_80
26. Madelung, O., U. Rossler, and M. Schulz. *Non-Tetrahedrally Bonded Elements and Binary Compounds I: Bismuth oxide (Bi₂O₃) crystal structure, chemical bond, lattice parameters*. Springer Berlin Heidelberg, 1998. Web. 27 July 2015, from http://link.springer.com/chapter/10.1007/10681727_80

27. Shannon, R. D. *Revised Effective Ionic Radii and Systematic Studies of Interatomic Distances in Halides and Chalcogenides*. Acta Crystallographica, 1976. Web. 4 July 2015, from <http://abulafia.mt.ic.ac.uk/shannon/>
28. Drozdov, A.P., Eremets, M.I., & Troyan, I.A. (2014). *Conventional superconductivity at 190 K at high pressures*.
29. Shen, K. M., & Davis, J.C. S. (n.d.). *Cuprate high-T_c superconductors*.
30. Blower, S., & Greaves, C. (1988). Bismuth additions to YBa₂Cu₃O₇: Structural and electrical characterisation. *Solid State Communications*, 765-767.
31. Dreuth, H., & Dederichs, H. (1993). Evaluation of low resistance contacts on YBa₂Cu₃O₇ thin films using the transmission line model. *Superconductor Science and Technology Supercond. Sci. Technol.*, 464-468.
32. Goyal, A. (n.d.). Epitaxial superconductors on rolling assisted biaxially textured substrates (RABiTS). 2.
33. Cockerham, Frey, Herrold, Johnson, Ko, Lucas, . . . Ru. (2007). *Effects on resistance and lattice structure using substitution-based superconductors*.